

Compact Finite Difference Scheme with Hermite Interpolation for Pricing American Put Options Based on Regime Switching Model

Chinonso I. Nwankwo^a, Weizhong Dai^{a,*}, Ruihua Liu^b

^a Department of Mathematics and Statistics, Louisiana Tech University, Ruston LA 71272, USA

^b Department of Mathematics, University of Dayton, 300 College Park, Dayton, OH 45469, USA

* Corresponding author, dai@coes.latech.edu

Abstract

We consider a system of coupled free boundary problems for pricing American put options with regime-switching. To solve this system, we first fix the optimal exercise boundary for each regime resulting in multi-variable fixed domains. We further eliminate the first-order derivatives associated with the regime-switching model by taking derivatives to obtain a system of coupled partial differential equations which we called the asset-delta-gamma-speed option equations. The fourth-order compact finite difference scheme is then employed in each regime for solving the system of the equations. In particular, the performance of cubic and quintic Hermite and cubic spline interpolation is explored in estimating the coupled asset, delta, gamma and speed options in the set of equations. The numerical method is finally tested with several examples. Our results show that the scheme provides an accurate solution with the convergent rate of 3.7 which is very fast in computation as compared with other existing numerical methods.

Keywords: American put options with regime switching, front-fixing transformation, optimal exercise boundary, compact finite difference method, Hermite interpolation

1. Introduction

The well-known Black-Scholes model has been used over decades in options valuation. This model constructs a delta hedging portfolio with an assumption of the frictionless market, no-arbitrage, and constant risk-free interest and volatility (Ugur, 2006). To remove this ideal assumption and reproduce the actual market price, risk, behavior, and dynamics, researchers have proposed several improvements by including stochastic volatility (Chockalingam and Muthuraman, 2011; Düring and Fournié, 2012; Garnier and Sølna, 2017; Huang et al., 2011; Hull and White, 1987; Ikonen and Toivanen, 2007; Zhylyevskyy, 2009),

jump-diffusion (Bingham, 2006; Chen et al., 2019; Cont and Tankov, 2004; Guoqing and Hanson, 2006; Kou, 2002), and regime-switching (Company et al, 2016a; Egorova et al., 2016; Huang et al., 2011; Khaliq and Liu, 2009; Mamon and Rodrigo, 2005) in the pricing models.

The regime-switching model for American option valuation, first introduced by Hamilton (1989), has gained broader interest after the seminal work of Buffington and Elliot (2002). It defines a finite number of market states known as regimes. Each regime has its own set of market variables, and the market randomly switches among different regimes (Chiarella et al., 2016). The model for option valuation with regime-switching involves a system of partial differential equations with free boundaries for which the analytical solution is very difficult to obtain in general. Thus, some works in the literature have proposed numerical techniques for solving the option pricing equation with regime-switching. Among them, the commonly known numerical methods are the penalty method (Khaliq and Liu, 2009; Nielsen et al., 2002; Zhang et al., 2013), the method of line (Chiarella et al., 2016; Meyer and van der Hoek, 1997), the lattice method (Han and Kim, 2016; Shang and Bryne, 2019), the fast Fourier transform (Boyarchenko and Levendorskii, 2008; Liu et al., 2006), and the front-fixing techniques (Egorova et al., 2016). The lattice-based method is more common among practitioners. However, tracking the optimal exercise boundary can be a challenge (Shang and Bryne, 2019). Fast Fourier transform method is efficient in solving the European options (Chiarella et al., 2016). The penalty method removes the free boundary by introducing a penalty term (Khaliq and Liu, 2009). MOL method calculates the asset and delta options and the optimal exercise boundary simultaneously during computation. Meyer and van der Hoek (1997) pointed out that there are still some complications with MOL method due to the singularity of the solution and infinite interval. The front-fixing technique (Blackwell and Hogan, 1994; Company et al., 2016b; Company et al., 2016c; Landau, 1950; Mitchell and Vynnycky, 2009; Mitchell and Vynnycky) was first applied by Egorova et al. (2016) to the regime-switching model.

To the best of our knowledge, the above methods provide up to second-order accurate solutions. The motivation of this research is to propose a highly accurate front-fixing numerical method for solving the regime-switching pricing model. To this end, we first use a logarithmic transformation to fix the optimal exercise boundary for each regime resulting in a multi-variable fixed domain. Furthermore, we remove the first-order derivative in the model by taking derivatives. As a result, the obtained system of the asset-delta-gamma-speed option equations can be discretized using a higher-order compact finite difference method coupled with high order interpolation methods. The discretized scheme is then solved using both

fixed-point and Newton iteration method, which predicts the optimal exercise boundary, option value and option Greeks in each regime.

The rest of the paper is organized as follows. In section 2, we consider a regime-switching model and its transformations. We transform the model to obtain coupled partial differential equations for option values, delta, gamma, and speed options in each regime. In section 3, we develop a numerical method and its algorithm for solving these equations and obtaining the option values, optimal exercise boundary and the Greeks in each regime. In section 4, we test our algorithm using examples with two, four, eight, and sixteen regimes. We conclude the paper in section 5.

2. Regime Switching Model and its Transformations

2.1. Regime Switching Model

Let us consider a continuous-time Markov chain whose states are labeled as $m = 1, 2, \dots, I$. Let $Q = (q_{ml})_{I \times I}$ represent the generator matrix with the entry elements q_{ml} satisfying the condition below (Norris, 1998):

$$q_{mm} = - \sum_{l \neq m} q_{ml}, \quad q_{ml} \geq 0, \quad \text{for } l \neq m, \quad l = 1, 2, \dots, I. \quad (1)$$

Assuming a risk-neutral measure (Elliot et al, 2007), the underlying asset follows a stochastic process

$$dS_t = S_t (r_{\alpha_t} dt + \sigma_{\alpha_t} dB_t), \quad 0 \leq t < \infty, \quad (2)$$

where r_{α_t} and σ_{α_t} are the interest rate and volatility of the asset, respectively, and are dependent on the Markov chain state with

$$r_{\alpha_t | \alpha_t} = r_m, \quad \sigma_{\alpha_t | \alpha_t} = \sigma_m, \quad m = 1, 2, \dots, I. \quad (3)$$

We consider an American put option written on the asset S_t with strike price K and expiration time T . Let $V_m(S, t)$ denote the option price and $\tau = T - t$. Then $V_m(S, t)$ satisfies the following parabolic PDEs with free boundaries:

$$-\frac{\partial V_m(S, \tau)}{\partial \tau} + \frac{1}{2} \sigma^2_m S^2 \frac{\partial^2 V_m(S, \tau)}{\partial S^2} + r_m S \frac{\partial V_m(S, \tau)}{\partial S} - r_m V_m(S, \tau) + \sum_{l \neq m} q_{ml} [V_l(S, \tau) - V_m(S, \tau)] = 0, \quad (4)$$

$$\text{for } S > s_{f(m)}(\tau),$$

$$V_m(S, \tau) = K - S, \quad \text{for } S < s_{f(m)}(\tau). \quad (5)$$

Here, the initial and boundary conditions are given as:

$$V_m(S, 0) = \max(K - S, 0), \quad s_{f(m)}(0) = K; \quad (6)$$

$$V_m(s_{f(m)}, \tau) = K - s_{f(m)}(\tau), \quad V_m(0, \tau) = K, \quad V_m(\infty, \tau) = 0, \quad \frac{\partial}{\partial S} V_m(s_{f(m)}, \tau) = -1, \quad (7)$$

where $s_{f(m)}(\tau)$ is the optimal exercise boundaries for each regime.

2.2. Logarithmic Multivariable Fixed Domain Transformation

To fix the free boundary challenge, we employ a transformation (Egorova, 2016; Wu and Kwok, 1997) on multi-variable domains as

$$x_m = \ln \frac{S}{s_{f(m)}(\tau)} = \ln S - \ln s_{f(m)}(\tau), \quad m = 1, 2, \dots, I, \quad (8)$$

where the variable x_m exists in a positive domain $x_m \in [0, \infty)$. The transformed m option value functions $U_m(x_m, \tau)$ are related to the original m option value functions $V_m(S, t)$ by the dimensionless transformation

$$U_m(x_m, \tau) = V_m(S, \tau), \quad m = 1, 2, \dots, I. \quad (9a)$$

Applying this transformation, we obtain the following relations:

$$\frac{\partial x_m}{\partial S} = \frac{1}{S}, \quad \frac{\partial x_m}{\partial \tau} = -\frac{s'_{f(m)}(\tau)}{s_{f(m)}(\tau)}, \quad \frac{\partial V_m}{\partial S} = \frac{1}{S} \frac{\partial U_m}{\partial x_m}; \quad (9b)$$

$$\frac{\partial^2 V_m}{\partial S^2} = \frac{1}{S^2} \left(-\frac{\partial U_m}{\partial x_m} + \frac{\partial^2 U_m}{\partial x_m^2} \right), \quad \frac{\partial V_m}{\partial \tau} = \left(\frac{\partial U_m}{\partial \tau} - \frac{s'_{f(m)}(\tau)}{s_{f(m)}(\tau)} \frac{\partial U_m}{\partial x_m} \right). \quad (9c)$$

Because our interest is to also calculate speed, delta decay, and color options, we differentiate further to obtain higher derivatives of the m option value functions as

$$\frac{\partial^3 V_m}{\partial S^3} = \frac{1}{S^3} \left(2 \frac{\partial U_m}{\partial x_m} - 3 \frac{\partial^2 U_m}{\partial x_m^2} + \frac{\partial^3 U_m}{\partial x_m^3} \right), \quad \frac{\partial^2 V_m}{\partial S \partial \tau} = \frac{1}{S} \left(\frac{\partial^2 U_m}{\partial x_m \partial \tau} - \frac{s'_{f(m)}(\tau)}{s_{f(m)}(\tau)} \frac{\partial^2 U_m}{\partial x_m^2} \right); \quad (9d)$$

$$\frac{\partial^3 V_m}{\partial S^2 \partial \tau} = \frac{1}{S^2} \left(\frac{\partial^3 U_m}{\partial x_m^2 \partial \tau} - \frac{\partial^2 U_m}{\partial x_m \partial \tau} + \frac{s'_{f(m)}(\tau)}{s_{f(m)}(\tau)} \frac{\partial^2 U_m}{\partial x_m^2} - \frac{s'_{f(m)}(\tau)}{s_{f(m)}(\tau)} \frac{\partial^3 U_m}{\partial x_m^3} \right). \quad (9e)$$

Let l represent the coupled regime(s) in the m free boundary PDE equations. The former also has a variable

$$x_l = \ln \frac{S}{s_{f(l)}(\tau)} = \ln S - \ln s_{f(l)}(\tau), \quad l \neq m, \quad l = 1, 2, \dots, I. \quad (10)$$

Eliminating S in the l^{th} and m^{th} equations, we obtain

$$x_l = x_m - \ln \frac{s_{f(l)}(\tau)}{s_{f(m)}(\tau)}. \quad (11)$$

Substituting (9) into (4), the model can be changed to

$$\begin{aligned} \frac{\partial U_m(x_m, \tau)}{\partial \tau} - \frac{1}{2} \sigma_m^2 \frac{\partial^2 U_m(x_m, \tau)}{\partial x_m^2} - \left(\frac{s'_{f(m)}}{s_{f(m)}} + r_m - \frac{\sigma_m^2}{2} \right) \frac{\partial U_m(x_m, \tau)}{\partial x_m} + r_m U_m(x_m, \tau) \\ - \sum_{l \neq m} q_{ml} [U_l(x_m, \tau) - U_m(x_m, \tau)] = 0, \quad \text{for } x_m > 0; \end{aligned} \quad (12)$$

$$U_m(x_m, \tau) = K - S = K - s_{f(m)}(\tau) e^{x_m}, \quad \text{for } x_m \leq 0; \quad (13)$$

$$\frac{\partial U_m(x_m, \tau)}{\partial x_m} = -s_{f(m)}(\tau) e^{x_m}, \quad \text{for } x_m \leq 0; \quad (14)$$

$$\frac{\partial U_m(x_m, \tau)}{\partial \tau} = -s'_{f(m)}(\tau) e^{x_m}, \quad \text{for } x_m \leq 0, \quad (15)$$

$$\frac{\partial^n U_m(x_m, \tau)}{\partial x_m^{n-1} \partial \tau} = -s'_{f(m)}(\tau) e^{x_m}, \quad \frac{\partial^n U_m(x_m, \tau)}{\partial x_m^n} = -s_{f(m)}(\tau) e^{x_m}, \quad \text{for } x_m \leq 0, \quad n > 0, \quad (16)$$

where the initial and boundary conditions are defined as:

$$U_m(x_m, 0) = \max[K(1 - e^{x_m}), 0], \quad s_{f(m)}(0) = K; \quad (17a)$$

$$U_m(0, \tau) = K - s_{f(m)}(\tau), \quad \frac{\partial U_m(0, \tau)}{\partial x_m} = -s_{f(m)}(\tau); \quad (17b)$$

$$\frac{\partial U_m(0, \tau)}{\partial \tau} = -s'_{f(m)}(\tau), \quad U_m(\infty, \tau) = 0. \quad (17c)$$

It should be pointed out that at $S = s_{f(m)}(\tau)$, $x_m = \ln 1 = 0$.

2.3. First, Second and Third Order Derivative Transformations

To apply the high order compact finite difference method, we further transform the system in (12)-(17) by eliminating the first-order derivative. To this end, we let $W_m(x_m, \tau)$ represent the derivative of the option value in each regime known as the delta option and given as

$$W_m(x_m, \tau) = \frac{\partial U_m(x_m, \tau)}{\partial x_m}. \quad (18)$$

Differentiating (12) with respect to x_m , we generate a coupled partial differential equation in terms of delta option of the form

$$\begin{aligned} \frac{\partial W_m(x_m, \tau)}{\partial \tau} - \frac{1}{2} \sigma_m^2 \frac{\partial^2 W_m(x_m, \tau)}{\partial x_m^2} - \left(\frac{s'_{f(m)}}{s_{f(m)}} + r_m - \frac{\sigma_m^2}{2} \right) \frac{\partial^2 U_m(x_m, \tau)}{\partial x_m^2} + r_m W_m(x_m, \tau) \\ - \sum_{l \neq m} q_{ml} (W_l(x_m, \tau) - W_m(x_m, \tau)) = 0, \quad \text{for } x_m > 0; \end{aligned} \quad (19)$$

$$W_m(x_m, \tau) = -s_{f(m)} e^{x_m}, \quad \text{for } x_m \leq 0; \quad (20)$$

where the initial and boundary conditions for $W_m(x_m, \tau)$ are defined as:

$$W_m(x_m, 0) = 0, \quad W_m(0, \tau) = -s_{f(m)}, \quad W_m(\infty, \tau) = 0. \quad (21)$$

Furthermore, we let $Y_m(x_m, \tau)$ represent the derivative of the delta option in each regime known as the gamma option and given as

$$Y_m(x_m, \tau) = \frac{\partial W_m(x_m, \tau)}{\partial x_m} = \frac{\partial^2 U_m(x_m, \tau)}{\partial x_m^2}. \quad (22)$$

Differentiating (19) with respect to x_m , we generate a coupled gamma option PDE equation for each regime of the form

$$\begin{aligned} \frac{\partial Y_m(x_m, \tau)}{\partial \tau} - \frac{1}{2} \sigma_m^2 \frac{\partial^2 Y_m(x_m, \tau)}{\partial x_m^2} - \left(\frac{s'_{f(m)}}{s_{f(m)}} + r_m - \frac{\sigma_m^2}{2} \right) \frac{\partial^2 W_m(x_m, \tau)}{\partial x_m^2} + r_m Y_m(x_m, \tau) \\ - \sum_{l \neq m} q_{ml} (Y_l(x_m, \tau) - Y_m(x_m, \tau)) = 0, \quad \text{for } x_m > 0; \end{aligned} \quad (23)$$

$$Y_m(x_m, \tau) = -s_{f(m)} e^{x_m}, \quad \text{for } x_m \leq 0; \quad (24)$$

where the initial and boundary conditions for $Y_m(x_m, \tau)$ are defined as

$$Y_m(x_m, 0) = 0, \quad Y_m(0, \tau) = -s_{f(m)}, \quad Y_m(\infty, \tau) = 0. \quad (25)$$

Finally, we let $Z_m(x_m, \tau)$ represent the derivative of the gamma option known as the speed option and given as

$$Z_m(x_m, \tau) = \frac{\partial Y_m(x_m, \tau)}{\partial x_m} = \frac{\partial^2 W_m(x_m, \tau)}{\partial x_m^2} = \frac{\partial^3 U_m(x_m, \tau)}{\partial x_m^3}. \quad (26)$$

Differentiating (23) with respect to x_m , we generate a coupled speed option PDE equation in each regime of the form

$$\begin{aligned} \frac{\partial Z_m(x_m, \tau)}{\partial \tau} - \frac{1}{2} \sigma_m^2 \frac{\partial^2 Z_m(x_m, \tau)}{\partial x_m^2} - \left(\frac{s'_{f(m)}}{s_{f(m)}} + r_m - \frac{\sigma_m^2}{2} \right) \frac{\partial^2 Y_m(x_m, \tau)}{\partial x_m^2} + r_m Z_m(x_m, \tau) \\ - \sum_{l \neq m} q_{ml} (Z_l(x_m, \tau) - Z_m(x_m, \tau)) = 0, \quad \text{for } x_m > 0; \end{aligned} \quad (27)$$

$$Z_m(x_m, \tau) = -s_{f(m)}e^{x_m}, \quad \text{for } x_m \leq 0; \quad (28)$$

where the initial and boundary conditions for $Z_m(x_m, \tau)$ are defined as:

$$Z_m(x_m, 0) = 0, \quad Z_m(0, \tau) = -s_{f(m)}, \quad Z_m(\infty, \tau) = 0. \quad (29)$$

Thus, a set of asset-delta-gamma-speed option PDE equations in each regime are obtained as follows:

$$\frac{\partial U_m}{\partial \tau} - \frac{1}{2}\sigma_m^2 \frac{\partial^2 U_m}{\partial x_m^2} - \left(\frac{s'_{f(m)}}{s_{f(m)}} + r_m - \frac{\sigma_m^2}{2} \right) W_m + (r_m - q_{mm})U_m - \sum_{l \neq m} q_{ml} U_l = 0, \quad (30a)$$

$$\frac{\partial W_m}{\partial \tau} - \frac{1}{2}\sigma_m^2 \frac{\partial^2 W_m}{\partial x_m^2} - \left(\frac{s'_{f(m)}}{s_{f(m)}} + r_m - \frac{\sigma_m^2}{2} \right) \frac{\partial^2 U_m}{\partial x_m^2} + (r_m - q_{mm})W_m - \sum_{l \neq m} q_{ml} W_l = 0, \quad (30b)$$

$$\frac{\partial Y_m}{\partial \tau} - \frac{1}{2}\sigma_m^2 \frac{\partial^2 Y_m}{\partial x_m^2} - \left(\frac{s'_{f(m)}}{s_{f(m)}} + r_m - \frac{\sigma_m^2}{2} \right) \frac{\partial^2 W_m}{\partial x_m^2} + (r_m - q_{mm})Y_m - \sum_{l \neq m} q_{ml} Y_l = 0, \quad (30c)$$

$$\frac{\partial Z_m}{\partial \tau} - \frac{1}{2}\sigma_m^2 \frac{\partial^2 Z_m}{\partial x_m^2} - \left(\frac{s'_{f(m)}}{s_{f(m)}} + r_m - \frac{\sigma_m^2}{2} \right) \frac{\partial^2 Y_m}{\partial x_m^2} + (r_m - q_{mm})Z_m - \sum_{l \neq m} q_{ml} Z_l = 0, \quad (30d)$$

where $m = 1, 2, \dots, I$, $x_m \in [0, \infty]$ and the initial and boundary conditions for $U_m(x_m, \tau)$, $W_m(x_m, \tau)$, $Y_m(x_m, \tau)$, and $Z_m(x_m, \tau)$ are defined as:

$$s_{f(m)}(0) = K, \quad U_m(x_m, 0) = 0, \quad W_m(x_m, 0) = 0, \quad Y_m(x_m, 0) = 0, \quad Z_m(x_m, 0) = 0; \quad (31a)$$

$$U_m(0, \tau) = K - s_{f(m)}(\tau), \quad W_m(0, \tau) = -s_{f(m)}(\tau), \quad Y_m(0, \tau) = -s_{f(m)}(\tau), \quad Z_m(0, \tau) = -s_{f(m)}(\tau); \quad (31b)$$

$$U_m(\infty, \tau) = 0; \quad W_m(\infty, \tau) = 0; \quad Y_m(\infty, \tau) = 0, \quad Z_m(\infty, \tau) = 0. \quad (31c)$$

It should be pointed out that finding the analytical solution for the above system could be quite troublesome, and therefore, it should be solved numerically.

3. Numerical Formulation

To solve the above asset-delta-gamma-speed option PDEs, we first design a uniform grid $[0, \infty) \times [0, T]$ for each regime taking into consideration how the m^{th} regime's domain relates to the l^{th} regime's domain using the Hermite interpolation technique. The infinite boundary is replaced with the far estimate boundary (Egorova et al, 2016; Kangro and Nicolaidis, 2000; Toivanen, 2010). which we denote as x_{fb} . Representing i as the node point in the m^{th} regime's domain, j as the node point in the l^{th} regime's domain and n as the time step. For a given positive integers M and N , representing the numbers of grid points and time steps, respectively, we have

$$(x_m)_i = ih, (x_l)_j = jh, \tau_n = nk, h = \frac{x_{fb}}{M}, k = \frac{T}{N}, i, j \in [0, M], k \in [0, N]. \quad (32)$$

We let the approximate solutions of $U_m((x_m)_i, \tau_n), U_l((x_m)_i, \tau_n), W_m((x_m)_i, \tau_n), W_l((x_m)_i, \tau_n), Y_m((x_m)_i, \tau_n), Z_m((x_m)_i, \tau_n)$, and $S_{f(m)}(\tau_n)$ to be $(u_m)_i^n, (u_l)_i^n, (w_m)_i^n, (w_l)_i^n, (y_m)_i^n, (z_m)_i^n$, and $S_{f(m)}^n$, respectively.

3.1. Numerical Discretization and Boundary Treatment

In the numerical discretization for the asset, delta, gamma and speed options in each regime, the fourth-order compact finite difference method is used in space, while the second-order Crank-Nicolson method is used in time. To be consistent with the Crank-Nicolson scheme in time, we choose not to freeze the n^{th} step in the coupled regime(s). To track the optimal exercise boundary in each regime, we reformulate the boundary condition for the asset option from (13)-(14) as follows:

$$\frac{\partial U_m(0, \tau)}{\partial x_m} - U_m(0, \tau) = W_m(0, \tau) - U_m(0, \tau) = -K. \quad (33)$$

Using the following compact finite difference scheme in space for boundary treatment (Gao and Sun, 2012; Liao and Khaliq, 2009; Yan et al, 2019; Zhao et al, 2007; Cao et al, 2011)

$$\frac{5}{12}f''(x_0) + \frac{1}{12}f''(x_1) = \frac{1}{h} \left[\frac{f(x_1) - f(x_0)}{h} - f'(x_0) \right] - \frac{h}{12}f'''(x_0) + O(h^3), \quad (34)$$

and the Crank-Nicolson method in time

$$f'(t_{n+1/2}) = \frac{1}{k} [f(t_{n+1}) - f(t_n)] + O(k^2), \quad (35)$$

the boundary condition for the asset option in each regime can be discretized from (30a). Applying (33) in (34), we then obtain

$$\begin{aligned} & -\frac{1}{2}\sigma^2 m \left[\frac{\partial^2 U_m(0, t_{n+1/2})}{\partial x_m^2} + \frac{\partial^2 U_m(1, t_{n+1/2})}{\partial x_m^2} \right] \\ & = \sigma^2 m \left[\frac{U_m(0, t_{n+1/2}) - U_m(1, t_{n+1/2})}{2h^2} \right] + \sigma^2 m \left[\frac{U_m(0, t_{n+1/2}) - K}{2h} \right] \\ & + \frac{\sigma^2 m h}{24} \frac{\partial^3 U_m(0, t_{n+1/2})}{\partial x_m^3}. \end{aligned} \quad (36)$$

Moreover, let

$$\omega_{n+1/2} \equiv \frac{2(S_{f(m)}^{n+1} - S_{f(m)}^n)}{k(S_{f(m)}^{n+1} + S_{f(m)}^n)} + r_m - \frac{\sigma^2 m}{2}, \quad \xi = q_{mm} - \frac{\sigma^2 m}{2}, \quad (37)$$

We can further evaluate the third derivative of the asset option in (36) by considering (30b) when $x = 0$ which we described as follow

$$\begin{aligned} & \frac{\sigma_m^2 h \partial^3 U_m(0, t_{n+1/2})}{24 \partial x_m^3} \\ &= \frac{h}{12} \left[\frac{[W_m(0, t_{n+1}) - W_m(0, t_n)]}{k} - \omega_{n+1/2} Y_m(0, t_{n+1/2}) + (r_m - q_{mm}) W_m(0, t_{n+1/2}) \right. \\ & \quad \left. - \sum_{l \neq m} q_{ml} W_l(0, t_{n+1/2}) \right] \end{aligned} \quad (38)$$

Also, it follows from (16) and (33) that

$$\frac{W_m(0, t_{n+1}) - W_m(0, t_n)}{k} = \frac{(U_m(0, t_{n+1}) - K) - (U_m(0, t_n) - K)}{k} = \frac{U_m(0, t_{n+1}) - U_m(0, t_n)}{k} \quad (39)$$

It is very important to point out that due to the coefficient term of the second derivative of asset option in (38), we could not adopt the equation

$$\frac{\sigma_m^2 \partial^2 U_m(0, t_{n+1/2})}{2 \partial x_m^2} = \xi W_m(0, t_{n+1/2}) + K(r_m - q_{mm}) - \sum_{l \neq m} q_{ml} U_l(0, t_{n+1/2}). \quad (40)$$

like the one shown in the work of Kwok (2008), Wu and Kwok (1997) and Company et al (2016) to evaluate $Y_m(0, t_{n+1/2})$ in (38). The reason is that our numerical scheme is sensitive to (40) and finds it hard to converge without implementing a damping factor (SUR). To overcome this challenge and avoid the use of the SUR iterative method, we then consider the classical fourth-order Hermitian approximation to a first derivative based on Pade Scheme (Adam, 1975) and used in the work of Liao and Khaliq (2009) and Dremkova and Ehrhardt (2011). Hence, the second derivative of the asset option when $x = 0$ is approximated as follows

$$Y_m(0, t_{n+1/2}) = \frac{3}{h} [W_m(2, t_{n+1/2}) - W_m(0, t_{n+1/2})] - 4Y_m(1, t_{n+1/2}) - Y_m(2, t_{n+1/2}) + O(h^4) \quad (41)$$

Our system of PDE equations provide solutions up to the third derivative of asset option which enables us to evaluate $Y_m(1, t_{n+1/2})$ and $Y_m(2, t_{n+1/2})$. Substituting (38) and (41) into (36), we then obtain

$$\begin{aligned} & -\frac{1}{2} \sigma_m^2 \left[\frac{\partial^2 U_m(0, t_{n+1/2})}{\partial x_m^2} + \frac{\partial^2 U_m(1, t_{n+1/2})}{\partial x_m^2} \right] \\ &= \sigma_m^2 \left[\frac{U_m(0, t_{n+1/2}) - U_m(1, t_{n+1/2})}{2h^2} \right] + \sigma_m^2 \left[\frac{U_m(0, t_{n+1/2}) - K}{2h} \right] \end{aligned}$$

$$\begin{aligned}
& + \frac{h}{12} \left[\frac{U_m(0, t_{n+1}) - U_m(0, t_n)}{k} \right] \\
& - \frac{h}{12} \omega_{n+1/2} \left(\frac{3}{h} W_m(2, t_{n+1/2}) - \frac{3}{h} W_m(0, t_{n+1/2}) - 4Y_m(1, t_{n+1/2}) - Y_m(2, t_{n+1/2}) \right) \\
& + \frac{h(r_m - q_{mm})}{12} U_m(0, t_{n+1/2}) - \frac{hK(r_m - q_{mm})}{12} \\
& - \sum_{l \neq m} q_{ml} W_l(0, t_{n+1/2})
\end{aligned} \tag{42a}$$

and the discretized boundary as

$$\begin{aligned}
& \frac{5+h}{12} \left[\frac{(u_m)_0^{n+1} - (u_m)_0^n}{k} \right] + \frac{1}{12} \left[\frac{(u_m)_1^{n+1} - (u_m)_1^n}{k} \right] - \frac{\sigma^2_m}{4h} \left[\frac{(u_m)_1^{n+1} - (u_m)_0^{n+1}}{h} - (u_m)_0^{n+1} \right] \\
& - \frac{\sigma^2_m}{4h} \left[\frac{(u_m)_1^n - (u_m)_0^n}{h} - (u_m)_0^n \right] - K \left[\frac{h(r_m - q_{mm})}{12} + \frac{\sigma^2_m}{2h} \right] \\
& + \frac{(r_m - q_{mm})}{24} [5 + h[(u_m)_0^{n+1} + (u_m)_0^n] + [(u_m)_1^{n+1} + (u_m)_1^n]] \\
& - \frac{\omega_{n+1/2}}{24} [2[(w_m)_0^{n+1} + (w_m)_0^n] + [(w_m)_1^{n+1} + (w_m)_1^n] + 3[(w_m)_2^{n+1} + (w_m)_2^n]] \\
& + \frac{h\omega_{n+1/2}}{24} [4[(y_m)_1^{n+1} + (y_m)_1^n] + [(y_m)_2^{n+1} + (y_m)_2^n]] - h \sum_{l \neq m} \frac{q_{ml}}{24} [(w_l)_0^{n+1} + (w_l)_0^n] \\
& - \sum_{l \neq m} \frac{q_{ml}}{24} [5[(u_l)_0^{n+1} + (u_l)_0^n] + [(u_l)_1^{n+1} + (u_l)_1^n]] = 0.
\end{aligned} \tag{42b}$$

As such, (42b) has a truncation error of $O(k^2 + h^3)$. At each interior grid point, using the compact finite difference scheme

$$\frac{1}{12} f''(x_{i-1}) + \frac{10}{12} f''(x_i) + \frac{1}{12} f''(x_{i+1}) = \frac{1}{h^2} [f(x_{i-1}) - 2f(x_i) + f(x_{i+1})] + O(h^4), \tag{43}$$

we discretize (30) as follows:

$$\begin{aligned}
& \frac{1}{12} \left[\frac{(u_m)_{i-1}^{n+1} - (u_m)_{i-1}^n}{k} \right] + \frac{10}{12} \left[\frac{(u_m)_i^{n+1} - (u_m)_i^n}{k} \right] + \frac{1}{12} \left[\frac{(u_m)_{i+1}^{n+1} - (u_m)_{i+1}^n}{k} \right] \\
& - \frac{\sigma^2_m}{4h^2} [(u_m)_{i-1}^{n+1} - 2(u_m)_i^{n+1} + (u_m)_{i+1}^{n+1}] - \frac{\sigma^2_m}{4h^2} [(u_m)_{i-1}^n - 2(u_m)_i^n + (u_m)_{i+1}^n] \\
& - \frac{\omega_{n+1/2}}{24} [(w_m)_{i-1}^{n+1} + (w_m)_{i-1}^n] + 10[(w_m)_i^{n+1} + (w_m)_i^n] + [(w_m)_{i+1}^{n+1} + (w_m)_{i+1}^n] \\
& + \frac{(r_m - q_{mm})}{24} [(u_m)_{i-1}^{n+1} + (u_m)_{i-1}^n] + 10[(u_m)_i^{n+1} + (u_m)_i^n] + [(u_m)_{i+1}^{n+1} + (u_m)_{i+1}^n] \\
& - \sum_{l \neq m} \frac{q_{ml}}{24} [(u_l)_{i-1}^{n+1} + (u_l)_{i-1}^n] + 10[(u_l)_i^{n+1} + (u_l)_i^n] + [(u_l)_{i+1}^{n+1} + (u_l)_{i+1}^n] \\
& = 0,
\end{aligned} \tag{44a}$$

$$\begin{aligned}
& \frac{1}{12} \left(\frac{(w_m)_{i-1}^{n+1} - (w_m)_{i-1}^n}{k} \right) + \frac{10}{12} \left(\frac{(w_m)_i^{n+1} - (w_m)_i^n}{k} \right) + \frac{1}{12} \left(\frac{(w_m)_{i+1}^{n+1} - (w_m)_{i+1}^n}{k} \right) \\
& - \frac{\sigma^2 m}{4h^2} [(w_m)_{i-1}^{n+1} - 2(w_m)_i^{n+1} + (w_m)_{i+1}^{n+1}] - \frac{\sigma^2 m}{4h^2} [(w_m)_{i-1}^n - 2(w_m)_i^n + (w_m)_{i+1}^n] \\
& - \frac{\omega_{n+1/2}}{2h^2} \left[[(u_m)_{i-1}^{n+1} + (u_m)_{i-1}^n] - 2[(u_m)_i^{n+1} + (u_m)_i^n] + [(u_m)_{i+1}^{n+1} + (u_m)_{i+1}^n] \right] \\
& + \frac{(r_m - q_{mm})}{24} \left[[(w_m)_{i-1}^{n+1} + (w_m)_{i-1}^n] + 10[(w_m)_i^{n+1} + (w_m)_i^n] + [(w_m)_{i+1}^{n+1} + (w_m)_{i+1}^n] \right] \\
& - \sum_{l \neq m} \frac{q_{ml}}{24} \left[[(w_l)_{i-1}^{n+1} + (w_l)_{i-1}^n] + 10[(w_l)_i^{n+1} + (w_l)_i^n] + [(w_l)_{i+1}^{n+1} + (w_l)_{i+1}^n] \right] \\
& = 0, \tag{44b}
\end{aligned}$$

$$\begin{aligned}
& \frac{1}{12} \left(\frac{(y_m)_{i-1}^{n+1} - (y_m)_{i-1}^n}{k} \right) + \frac{10}{12} \left(\frac{(y_m)_i^{n+1} - (y_m)_i^n}{k} \right) + \frac{1}{12} \left(\frac{(y_m)_{i+1}^{n+1} - (y_m)_{i+1}^n}{k} \right) \\
& - \frac{\sigma^2 m}{4h^2} [(y_m)_{i-1}^{n+1} - 2(y_m)_i^{n+1} + (y_m)_{i+1}^{n+1}] - \frac{\sigma^2 m}{4h^2} [(y_m)_{i-1}^n - 2(y_m)_i^n + (y_m)_{i+1}^n] \\
& - \frac{\omega_{n+1/2}}{2h^2} \left[[(y_m)_{i-1}^{n+1} + (y_m)_{i-1}^n] - 2[(y_m)_i^{n+1} + (y_m)_i^n] + [(y_m)_{i+1}^{n+1} + (y_m)_{i+1}^n] \right] \\
& + \frac{(r_m - q_{mm})}{24} \left[[(y_m)_{i-1}^{n+1} + (y_m)_{i-1}^n] + 10[(y_m)_i^{n+1} + (y_m)_i^n] + [(y_m)_{i+1}^{n+1} + (y_m)_{i+1}^n] \right] \\
& - \sum_{l \neq m} \frac{q_{ml}}{24} \left[[(y_l)_{i-1}^{n+1} + (y_l)_{i-1}^n] + 10[(y_l)_i^{n+1} + (y_l)_i^n] + [(y_l)_{i+1}^{n+1} + (y_l)_{i+1}^n] \right] \\
& = 0, \tag{44c}
\end{aligned}$$

$$\begin{aligned}
& \frac{1}{12} \left(\frac{(z_m)_{i-1}^{n+1} - (z_m)_{i-1}^n}{k} \right) + \frac{10}{12} \left(\frac{(z_m)_i^{n+1} - (z_m)_i^n}{k} \right) + \frac{1}{12} \left(\frac{(z_m)_{i+1}^{n+1} - (z_m)_{i+1}^n}{k} \right) \\
& - \frac{\sigma^2 m}{4h^2} [(z_m)_{i-1}^{n+1} - 2(z_m)_i^{n+1} + (z_m)_{i+1}^{n+1}] - \frac{\sigma^2 m}{4h^2} [(z_m)_{i-1}^n - 2(z_m)_i^n + (z_m)_{i+1}^n] \\
& - \frac{\omega_{n+1/2}}{2h^2} \left[[(z_m)_{i-1}^{n+1} + (z_m)_{i-1}^n] - 2[(z_m)_i^{n+1} + (z_m)_i^n] + [(z_m)_{i+1}^{n+1} + (z_m)_{i+1}^n] \right] \\
& + \frac{(r_m - q_{mm})}{24} \left[[(z_m)_{i-1}^{n+1} + (z_m)_{i-1}^n] + 10[(z_m)_i^{n+1} + (z_m)_i^n] + [(z_m)_{i+1}^{n+1} + (z_m)_{i+1}^n] \right] \\
& - \sum_{l \neq m} \frac{q_{ml}}{24} \left[[(z_l)_{i-1}^{n+1} + (z_l)_{i-1}^n] + 10[(z_l)_i^{n+1} + (z_l)_i^n] + [(z_l)_{i+1}^{n+1} + (z_l)_{i+1}^n] \right] \\
& = 0, \tag{44d}
\end{aligned}$$

where $i = 1, 2, \dots, M - 1$ and $n = 1, 2, \dots, N$. Here, the truncation error is $O(k^2 + h^4)$. The optimal exercise boundary and the initial and boundary conditions for each regime are calculated as

$$s_{f(m)}^{n+1} = K - (u_m)_0^{n+1}, \quad (w_m)_0^{n+1} = -s_{f(m)}^{n+1}, \quad (y_m)_0^{n+1} = -s_{f(m)}^{n+1}, \quad (z_m)_0^{n+1} = -s_{f(m)}^{n+1}; \quad (45a)$$

$$(u_m)_M^{n+1} = 0, \quad (w_m)_M^{n+1} = 0, \quad (y_m)_M^{n+1} = 0, \quad (z_m)_M^{n+1} = 0; \quad (45b)$$

$$(u_m)_i^0 = (w_m)_i^0 = (y_m)_i^0 = (z_m)_i^0 = 0, \quad i = 1, 2, \dots, M. \quad (45c)$$

Let the approximate solutions of the theta, delta decay, and color options for each regime be given as

$$\frac{\partial U_m((x_m)_i, \tau_n)}{\partial \tau} \approx (\Theta_m)_i^n; \quad \frac{\partial W_m((x_m)_i, \tau_n)}{\partial \tau} \approx (K_m)_i^n; \quad \frac{\partial Y_m((x_m)_i, \tau_n)}{\partial \tau} \approx (\Gamma_m)_i^n, \quad (46)$$

respectively. For $n = 1$, we approximate the three Greeks using the first-order backward finite difference

$$(\Theta_m)_i^1 = \frac{(u_m)_i^1 - (u_m)_i^0}{k}, \quad (K_m)_i^1 = \frac{(w_m)_i^1 - (w_m)_i^0}{k}, \quad (\Gamma_m)_i^1 = \frac{(y_m)_i^1 - (y_m)_i^0}{k}. \quad (47a)$$

Subsequently, we use the second-order backward finite difference approximations

$$(\Theta_m)_i^{n+1} = \frac{3(u_m)_i^{n+1} - 4(u_m)_i^n + (u_m)_i^{n-1}}{2k}, \quad (K_m)_i^{n+1} = \frac{3(w_m)_i^{n+1} - 4(w_m)_i^n + (w_m)_i^{n-1}}{2k}; \quad (47b)$$

$$(\Gamma_m)_i^{n+1} = \frac{3(y_m)_i^{n+1} - 4(y_m)_i^n + (y_m)_i^{n-1}}{2k}, \quad (47c)$$

where k represents the time step. The initial conditions of the theta, delta decay and color options for each regime are calculated as

$$(\Theta_m)_i^0 = 0; \quad (K_m)_i^0 = 0, \quad (\Gamma_m)_i^0 = 0, \quad i = 0, 1, \dots, M. \quad (48)$$

3.2. Hermite Interpolation and Multi-Variable Domain Relationship

Since the mesh for the l^{th} regime may not completely overlap with the mesh for the m^{th} regime, we need to consider the relationship between these two fixed domains as shown in Fig. 1 in order to evaluate $(u_l)_i^n, (w_l)_i^n, (y_l)_i^n$ and $(z_l)_i^n$. It is important to note that $(u_l)_i^n \equiv (u_l)_{j^*}^n$ and $(w_l)_i^n \equiv (w_l)_{j^*}^n, (y_l)_i^n \equiv (y_l)_{j^*}^n, (z_l)_i^n \equiv (z_l)_{j^*}^n$ and $(x_l)_{j^*} \equiv (x_l)_i$.

From Fig. 1, we see that if $s_{f(l)}^n = s_{f(m)}^n$, then we have $(x_l)_{j^*} = (x_m)_i$. If $s_{f(l)}^n > s_{f(m)}^n$, the natural log of their ratio (with $s_{f(l)}^n$ as the numerator) becomes strictly positive. With respect to $(x_m)_i$, as shown in Fig. 1a, there exists a possibility for $(x_l)_{j^*} < 0$ which forces the l^{th} domain to have a negative real line. For this case, $(u_l)_i^n = K - s_{f(l)}^n e^{(x_l)_{j^*}}$ and $(w_l)_i^n = (y_l)_i^n = (z_l)_i^n = -s_{f(l)}^n e^{(x_l)_{j^*}}$ based on (13)-(16). If $(x_l)_{j^*} > 0$, as shown in Fig. 1(b), $(u_l)_i^n, (w_l)_i^n, (y_l)_i^n$ and $(z_l)_i^n$ have to be obtained using an interpolation technique. Because $(u_l)_j^n, (w_l)_j^n, (y_l)_j^n$ and $(z_l)_j^n$ are already known, it is convenient to employ the Hermite

interpolation (Burden et al, 2016) to evaluate $(u_l)_i^n, (w_l)_i^n, (y_l)_i^n$ and $(z_l)_i^n$. If $(x_l)_{j^*} > x_{fb}$ which is beyond the l^{th} domain, we then set $(u_l)_i^n = (w_l)_i^n = (y_l)_i^n = (z_l)_i^n = 0$ as shown in Fig. 1(c). As such, we have the following relationship for $(u_l)_i^n, (w_l)_i^n, (y_l)_i^n$ and $(z_l)_i^n$ as:

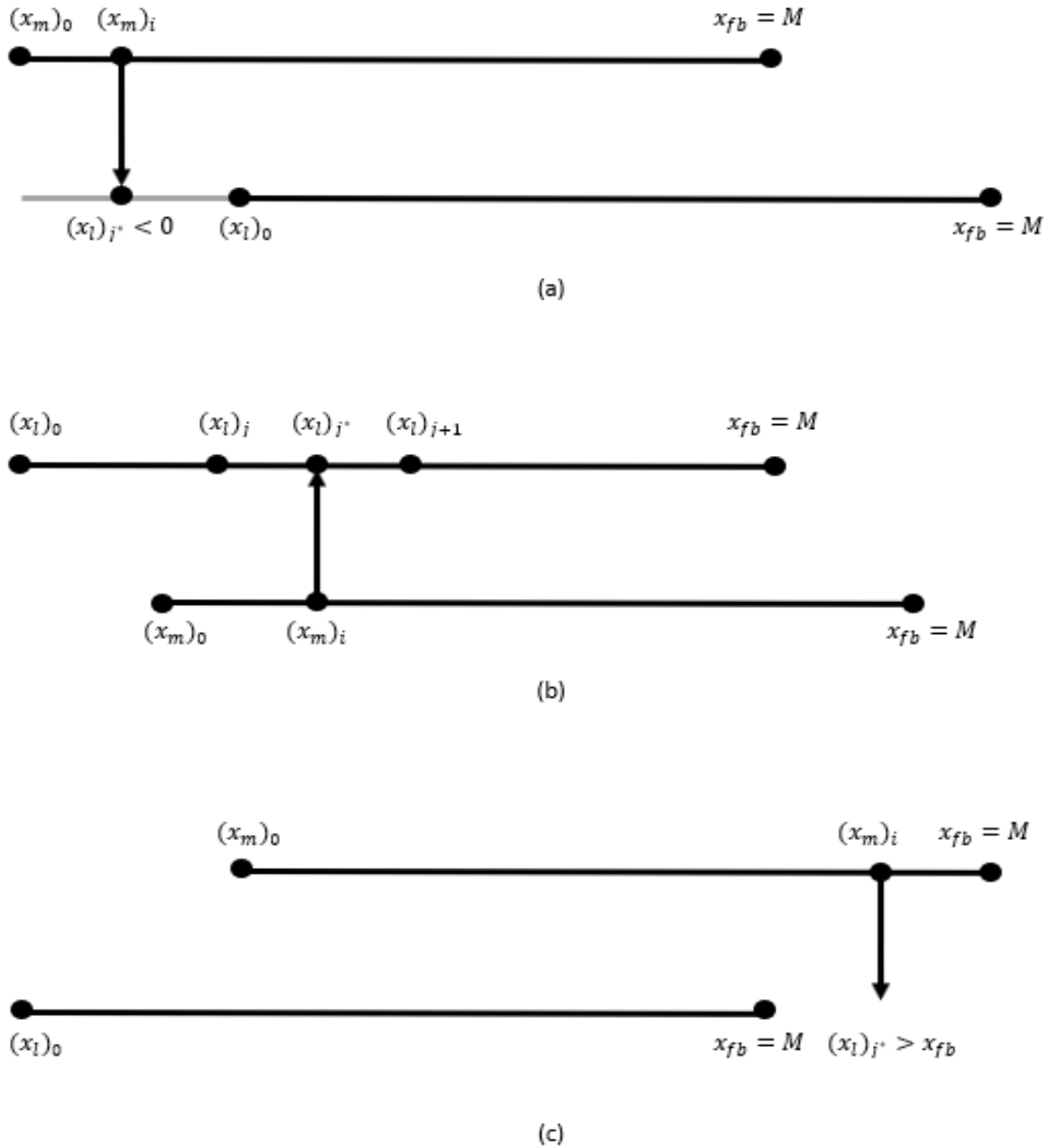


Fig. 1. Relationship between the l^{th} and m^{th} domains.

$$(u)_i^n = \begin{cases} K - s_{f(l)}(t_n)e^{(x_l)_i}, & (x_m)_i - \ln \frac{s_{f(l)}(t_n)}{s_{f(m)}(t_n)} \leq 0; \\ g(u_l)_j^n + m(u_l)_{j+1}^n + n(w_l)_j^n + o(w_l)_j^n, & (x_l)_j \leq (x_m)_i - \ln \frac{s_{f(l)}(t_n)}{s_{f(m)}(t_n)} \leq (x_l)_{j+1}; \\ 0, & (x_m)_i - \ln \frac{s_{f(l)}(t_n)}{s_{f(m)}(t_n)} > x_{fb}, \end{cases} \quad (49a)$$

$$(w)_i^n = \begin{cases} -s_{f(l)}(t_n)e^{(x_l)_i}, & (x_m)_i - \ln \frac{s_{f(l)}(t_n)}{s_{f(m)}(t_n)} \leq 0; \\ g(u_l)_j^n + m(u_l)_{j+1}^n + n(w_l)_j^n + o(w_l)_j^n, & (x_l)_j \leq (x_m)_i - \ln \frac{s_{f(l)}(t_n)}{s_{f(m)}(t_n)} \leq (x_l)_{j+1}; \\ 0, & (x_m)_i - \ln \frac{s_{f(l)}(t_n)}{s_{f(m)}(t_n)} > x_{fb}, \end{cases} \quad (49b)$$

$$(y)_i^n = \begin{cases} -s_{f(l)}(t_n)e^{(x_l)_i}, & (x_m)_i - \ln \frac{s_{f(l)}(t_n)}{s_{f(m)}(t_n)} \leq 0; \\ g(y_l)_j^n + m(y_l)_{j+1}^n + n(z_l)_j^n + o(z_l)_j^n, & (x_l)_j \leq (x_m)_i - \ln \frac{s_{f(l)}(t_n)}{s_{f(m)}(t_n)} \leq (x_l)_{j+1}; \\ 0, & (x_m)_i - \ln \frac{s_{f(l)}(t_n)}{s_{f(m)}(t_n)} > x_{fb}, \end{cases} \quad (49c)$$

$$(z)_i^n = \begin{cases} -s_{f(l)}(t_n)e^{(x_l)_i}, & (x_m)_i - \ln \frac{s_{f(l)}(t_n)}{s_{f(m)}(t_n)} \leq 0; \\ g(z_l)_j^n + m(z_l)_{j+1}^n + n(\dot{z})_j^n + o(\dot{z})_j^n, & (x_l)_j \leq (x_m)_i - \ln \frac{s_{f(l)}(t_n)}{s_{f(m)}(t_n)} \leq (x_l)_{j+1}; \\ 0, & (x_m)_i - \ln \frac{s_{f(l)}(t_n)}{s_{f(m)}(t_n)} > x_{fb}, \end{cases} \quad (49d)$$

where the following coefficients are given based on the cubic Hermite Interpolation (Burden et al, 2016)

$$g = \frac{1}{h^2} \left[1 + \frac{2[(x_l)_{j^*} - (x_l)_j]}{h} \right] [(x_l)_{j^*} - (x_l)_{j+1}]^2, \quad (49e)$$

$$h = \frac{1}{h^2} \left[1 - \frac{2[(x_l)_{j^*} - (x_l)_{j+1}]}{h} \right] [(x_l)_{j^*} - (x_l)_j]^2, \quad (49f)$$

$$i = \frac{1}{h^2} [(x_l)_{j^*} - (x_l)_j] [(x_l)_{j^*} - (x_l)_{j+1}]^2, \quad (49g)$$

$$j = \frac{1}{h^2} [(x_l)_{j^*} - (x_l)_{j+1}] [(x_l)_{j^*} - (x_l)_j]^2, \quad (49h)$$

For quintic Hermite Interpolation, we have the following relationship:

$$(u_l)_i^n = \begin{cases} K - s_{f(l)}^n e^{(x_l)_i}, & (x_m)_i - \ln \frac{S_{f(l)}^n}{S_{f(m)}^n} \leq 0; \\ a(u_l)_{j-1}^n + b(u_l)_j^n + c(u_l)_{j+1}^n + d(w_l)_{j-1}^n + e(w_l)_j^n, \dots \\ \dots + f(w_l)_{j+1}^n, & (x_l)_j \leq (x_m)_i - \ln \frac{S_{f(l)}^n}{S_{f(m)}^n} \leq (x_l)_{j+1}; \\ 0, & (x_m)_i - \ln \frac{S_{f(l)}^n}{S_{f(m)}^n} > x_{fb}, \end{cases} \quad (49i)$$

$$(w_l)_i^n = \begin{cases} -s_{f(l)}^n e^{(x_l)_i}, & (x_m)_i - \ln \frac{S_{f(l)}^n}{S_{f(m)}^n} \leq 0; \\ a(w_l)_{j-1}^n + b(w_l)_j^n + c(w_l)_{j+1}^n + d(y_l)_{j-1}^n + e(y_l)_j^n, \dots \\ \dots + f(y_l)_{j+1}^n, & (x_l)_j \leq (x_m)_i - \ln \frac{S_{f(l)}^n}{S_{f(m)}^n} \leq (x_l)_{j+1}; \\ 0, & (x_m)_i - \ln \frac{S_{f(l)}^n}{S_{f(m)}^n} > x_{fb}, \end{cases} \quad (49j)$$

$$(y_l)_i^n = \begin{cases} -s_{f(l)}^n e^{(x_l)_i}, & (x_m)_i - \ln \frac{S_{f(l)}^n}{S_{f(m)}^n} \leq 0; \\ a(y_l)_{j-1}^n + b(y_l)_j^n + c(y_l)_{j+1}^n + d(z_l)_{j-1}^n + e(z_l)_j^n, \dots \\ \dots + f(z_l)_{j+1}^n, & (x_l)_j \leq (x_m)_i - \ln \frac{S_{f(l)}^n}{S_{f(m)}^n} \leq (x_l)_{j+1}; \\ 0, & (x_m)_i - \ln \frac{S_{f(l)}^n}{S_{f(m)}^n} > x_{fb}, \end{cases} \quad (49k)$$

$$(z_l)_i^n = \begin{cases} -s_{f(l)}^n e^{(x)_i}, & (x_m)_i - \ln \frac{S_{f(l)}^n}{S_{f(m)}^n} \leq 0; \\ a(z_l)_{j-1}^n + b(z_l)_j^n + c(z_l)_{j+1}^n + d(\dot{z}_l)_{j-1}^n + e(\dot{z}_l)_j^n, \dots \\ \dots + f(\dot{z}_l)_{j+1}^n, & (x_l)_j \leq (x_m)_i - \ln \frac{S_{f(l)}^n}{S_{f(m)}^n} \leq (x_l)_{j+1}; \\ 0, & (x_m)_i - \ln \frac{S_{f(l)}^n}{S_{f(m)}^n} > x_{fb}, \end{cases} \quad (49l)$$

with the coefficients given as

$$a = \left[1 + \frac{3}{h}(x - x_{i-1}) \right] \frac{[(x - x_i)(x - x_{i+1})]^2}{4h^4}, \quad (49m)$$

$$b = \frac{[(x - x_{i-1})(x - x_{i+1})]^2}{h^4}, \quad (49n)$$

$$c = \left[1 - \frac{3}{h}(x - x_{i+1}) \right] \frac{[(x - x_{i-1})(x - x_i)]^2}{4h^4}, \quad (49o)$$

$$d = (x - x_{i-1}) \frac{[(x - x_i)(x - x_{i+1})]^2}{4h^4}, \quad (49p)$$

$$e = (x - x_i) \frac{[(x - x_{i-1})(x - x_{i+1})]^2}{h^4}, \quad (49q)$$

$$f = (x - x_{i+1}) \frac{[(x - x_{i-1})(x - x_i)]^2}{4h^4}. \quad (49r)$$

Note that $(\dot{z})_j^n$ denotes the derivative of $(z)_j^n$. To carry out an extensive analysis, we further investigate the performance of both cubic and quintic Hermite interpolation in the numerical example section using both fixed point and Newton iteration method.

3.3. Stability Analysis

The stability analysis of our numerical schemes is carried out using the matrix form of von Neumann method (see Hirsch (2001) and Liao and Khaliq (2009)). Due to the complex system of the present method, we ignore the coupled regimes $(u_l)_i^n$ and $(w_l)_i^n$, $(y_l)_i^n$ and $(z_l)_i^n$. Let

$$(u_m)_i^n = \lambda_m^n e^{I\beta i h}, \quad (w_m)_i^n = \Phi_m^n e^{I\beta i h}, \quad (y_m)_i^n = \Upsilon_m^n e^{I\beta i h}, \quad (z_m)_i^n = \Psi_m^n e^{I\beta i h}, \quad I = \sqrt{-1}. \quad (50)$$

Denote

$$\mu = \frac{\sigma_m^2 k}{4h^2}, \quad \kappa = (r_m - q_{mm})k, \quad \omega = \left(\frac{2(s_{f(m)}^{n+1} - s_{f(m)}^n)}{(s_{f(m)}^{n+1} + s_{f(m)}^n)} + r_m - \frac{\sigma_m^2}{2} \right) k. \quad (51)$$

Substituting (50) and (51) into (43a), (43b), (43c), and (43d), we obtain

$$\begin{aligned} & \lambda_m^{n+1} \left[1 - \frac{1}{3} \sin^2 \left(\frac{\beta h}{2} \right) + 4\mu \sin^2 \left(\frac{\beta h}{2} \right) + \frac{\kappa}{2} - \frac{\kappa}{2} \sin^2 \left(\frac{\beta h}{2} \right) \right] \\ & - \lambda_m^n \left[1 - \frac{1}{3} \sin^2 \left(\frac{\beta h}{2} \right) - 4\mu \sin^2 \left(\frac{\beta h}{2} \right) + \frac{\kappa}{2} - \frac{\kappa}{2} \sin^2 \left(\frac{\beta h}{2} \right) \right] \\ & - \omega \left[\Phi_m^{n+1} \left(\frac{1}{2} - \frac{1}{6} \sin^2 \left(\frac{\beta h}{2} \right) \right) + \Phi_m^n \left(\frac{1}{2} - \frac{1}{6} \sin^2 \left(\frac{\beta h}{2} \right) \right) \right] = 0, \end{aligned} \quad (52a)$$

$$\begin{aligned} & \Phi_m^{n+1} \left[1 - \frac{1}{3} \sin^2 \left(\frac{\beta h}{2} \right) + 4\mu \sin^2 \left(\frac{\beta h}{2} \right) + \frac{\kappa}{2} - \frac{\kappa}{2} \sin^2 \left(\frac{\beta h}{2} \right) \right] \\ & - \Phi_m^n \left[1 - \frac{1}{3} \sin^2 \left(\frac{\beta h}{2} \right) - 4\mu \sin^2 \left(\frac{\beta h}{2} \right) + \frac{\kappa}{2} - \frac{\kappa}{2} \sin^2 \left(\frac{\beta h}{2} \right) \right] \\ & - \omega \left[-4\lambda_m^{n+1} \sin^2 \left(\frac{\beta h}{2} \right) - 4\lambda_m^n \sin^2 \left(\frac{\beta h}{2} \right) \right] = 0, \end{aligned} \quad (52b)$$

$$\begin{aligned} & \Upsilon_m^{n+1} \left[1 - \frac{1}{3} \sin^2 \left(\frac{\beta h}{2} \right) + 4\mu \sin^2 \left(\frac{\beta h}{2} \right) + \frac{\kappa}{2} - \frac{\kappa}{2} \sin^2 \left(\frac{\beta h}{2} \right) \right] \\ & - \Upsilon_m^n \left[1 - \frac{1}{3} \sin^2 \left(\frac{\beta h}{2} \right) - 4\mu \sin^2 \left(\frac{\beta h}{2} \right) + \frac{\kappa}{2} - \frac{\kappa}{2} \sin^2 \left(\frac{\beta h}{2} \right) \right] \\ & - \omega \left[-4\Phi_m^{n+1} \sin^2 \left(\frac{\beta h}{2} \right) - 4\Phi_m^n \sin^2 \left(\frac{\beta h}{2} \right) \right] = 0, \end{aligned} \quad (52c)$$

$$\begin{aligned} & \Psi_m^{n+1} \left[1 - \frac{1}{3} \sin^2 \left(\frac{\beta h}{2} \right) + 4\mu \sin^2 \left(\frac{\beta h}{2} \right) + \frac{\kappa}{2} - \frac{\kappa}{2} \sin^2 \left(\frac{\beta h}{2} \right) \right] \\ & - \Psi_m^n \left[1 - \frac{1}{3} \sin^2 \left(\frac{\beta h}{2} \right) - 4\mu \sin^2 \left(\frac{\beta h}{2} \right) + \frac{\kappa}{2} - \frac{\kappa}{2} \sin^2 \left(\frac{\beta h}{2} \right) \right] \\ & - \omega \left[-4\Upsilon_m^{n+1} \sin^2 \left(\frac{\beta h}{2} \right) - 4\Upsilon_m^n \sin^2 \left(\frac{\beta h}{2} \right) \right] = 0, \end{aligned} \quad (52d)$$

which can be simplified to

$$p\lambda_m^{n+1} - q\lambda_m^n = r\Phi_m^{n+1} + r\Phi_m^n, \quad p\Phi_m^{n+1} - q\Phi_m^n = s\lambda_m^{n+1} + s\lambda_m^n; \quad (53a)$$

$$p\Upsilon_m^{n+1} - q\Upsilon_m^n = s\Phi_m^{n+1} + s\Phi_m^n, \quad p\Psi_m^{n+1} - q\Psi_m^n = s\Upsilon_m^{n+1} + s\Upsilon_m^n, \quad (53b)$$

where

$$p = \left[1 - \frac{1}{3} \sin^2 \left(\frac{\beta h}{2} \right) + 4\mu \sin^2 \left(\frac{\beta h}{2} \right) + \frac{\kappa}{2} - \frac{\kappa}{2} \sin^2 \left(\frac{\beta h}{2} \right) \right], \quad r = -\frac{2\omega}{h^2} \sin^2 \left(\frac{\beta h}{2} \right); \quad (54a)$$

$$s = \omega \left[\frac{1}{2} - \frac{1}{6} \sin^2 \left(\frac{\beta h}{2} \right) \right], \quad q = \left[1 - \frac{1}{3} \sin^2 \left(\frac{\beta h}{2} \right) - 4\mu \sin^2 \left(\frac{\beta h}{2} \right) + \frac{\kappa}{2} - \frac{\kappa}{2} \sin^2 \left(\frac{\beta h}{2} \right) \right]. \quad (54b)$$

We then obtain a system of equations from (52) as

$$\begin{bmatrix} \lambda_m^{n+1} \\ \Phi_m^{n+1} \\ \Upsilon_m^{n+1} \\ \Psi_m^{n+1} \end{bmatrix} = \begin{bmatrix} p & -r & 0 & 0 \\ -s & p & 0 & 0 \\ 0 & -s & p & 0 \\ 0 & 0 & -s & p \end{bmatrix}^{-1} \begin{bmatrix} q & r & 0 & 0 \\ s & q & 0 & 0 \\ 0 & s & q & 0 \\ 0 & 0 & s & q \end{bmatrix} \begin{bmatrix} \lambda_m^n \\ \Phi_m^n \\ \Upsilon_m^n \\ \Psi_m^n \end{bmatrix}, \quad (55a)$$

$$\begin{bmatrix} \lambda_m^{n+1} \\ \Phi_m^{n+1} \\ \Upsilon_m^{n+1} \\ \Psi_m^{n+1} \end{bmatrix} = \begin{bmatrix} \frac{p}{p^2 - sr} & \frac{r}{p^2 - sr} & 0 & 0 \\ \frac{s}{p^2 - sr} & \frac{p}{p^2 - sr} & 0 & 0 \\ \frac{s^2}{p(p^2 - sr)} & \frac{s}{p^2 - sr} & \frac{1}{p} & 0 \\ \frac{s^3}{p^2(p^2 - sr)} & \frac{s^2}{p(p^2 - sr)} & \frac{s}{p^2} & \frac{1}{p} \end{bmatrix} \begin{bmatrix} q & r & 0 & 0 \\ s & q & 0 & 0 \\ 0 & s & q & 0 \\ 0 & 0 & s & q \end{bmatrix} \begin{bmatrix} \lambda_m^n \\ \Phi_m^n \\ \Upsilon_m^n \\ \Psi_m^n \end{bmatrix}, \quad (55b)$$

$$\begin{bmatrix} \lambda_m^{n+1} \\ \Phi_m^{n+1} \\ \Upsilon_m^{n+1} \\ \Psi_m^{n+1} \end{bmatrix} = \begin{bmatrix} \frac{pq + rs}{p^2 - sr} & \frac{pr + qr}{p^2 - sr} & 0 & 0 \\ \frac{ps + qs}{p^2 - sr} & \frac{pq + rs}{p^2 - sr} & 0 & 0 \\ \frac{ps^2 + qs^2}{p(p^2 - sr)} & \frac{pqs + p^2s}{p(p^2 - sr)} & \frac{q}{p} & 0 \\ \frac{ps^3 + qs^3}{p^2(p^2 - sr)} & \frac{pqs^2 + p^2s^2}{p^2(p^2 - sr)} & \frac{ps + qs}{p^2} & \frac{q}{p} \end{bmatrix} \begin{bmatrix} \lambda_m^n \\ \Phi_m^n \\ \Upsilon_m^n \\ \Psi_m^n \end{bmatrix} = A \begin{bmatrix} \lambda_m^n \\ \Phi_m^n \\ \Upsilon_m^n \\ \Psi_m^n \end{bmatrix}. \quad (55c)$$

Here, A represents the amplification matrix. To show that our numerical method is unconditionally stable, we need to confirm that the modulus of the eigenvalue of the matrix A is less than or equal to 1 (see Hirsch (2001) and Liao and Khaliq (2009)). Representing the eigenvalue of the matrix A as β , we obtain the equation below

$$\left[\beta^2 - 2\beta \frac{pq + rs}{p^2 - sr} + \frac{(pq + rs)^2}{(p^2 - sr)^2} - \frac{(pr + qr)(ps + qs)}{(p^2 - sr)^2} \right] \left[\left(\frac{q}{p} - \beta \right) \left(\frac{q}{p} - \beta \right) \right] = 0. \quad (56)$$

Note that

$$rs = -\frac{2\omega^2}{h^2} \sin^2\left(\frac{\beta h}{2}\right) \left[\frac{1}{2} - \frac{1}{6} \sin^2\left(\frac{\beta h}{2}\right) \right] \leq 0, \quad p \geq q. \quad (57)$$

When $\mu > 0$, we obtain $p > q$ and hence, for

$$\left[\left(\frac{q}{p} - \beta \right) \left(\frac{q}{p} - \beta \right) \right] = 0, \quad |\beta_{1,2}| = \left| \frac{q}{p} \right| < 1. \quad (58)$$

Furthermore, we need to obtain $\beta_{3,4}$ by solving

$$\left[\beta^2 - 2\beta \frac{pq + rs}{p^2 - sr} + \frac{(pq + rs)^2}{(p^2 - sr)^2} - \frac{(pr + qr)(ps + qs)}{(p^2 - sr)^2} \right] = 0. \quad (59)$$

The solutions of (59) are presented as

$$\beta_{3,4} = \frac{(pq + rs) \pm (p + q)\sqrt{rs}}{p^2 - rs}. \quad (60)$$

Denoting $\varpi = -rs \geq 0$, we obtain the complex conjugate values of the eigenvalues as

$$\beta_{3,4} = \frac{(pq - \varpi) \pm (p + q)I\sqrt{\varpi}}{p^2 + \varpi}. \quad (61a)$$

To confirm unconditional stability, we need to show that $|\beta_{3,4}|^2 \leq 1$.

$$|\beta_{3,4}|^2 = \frac{(pq - \varpi)^2 + (p + q)^2\varpi}{(p^2 + \varpi)^2} = \frac{p^2q^2 - 2\varpi pq + \varpi^2 + \varpi p^2 + 2\varpi pq + \varpi q^2}{(p^2 + \varpi)^2}. \quad (61b)$$

Simplifying further, we obtain

$$|\beta_{3,4}|^2 = \frac{\varpi^2 + \varpi(p^2 + q^2) + p^2q^2}{(p^2 + \varpi)^2} = \frac{(p^2 + \varpi)(q^2 + \varpi)}{(p^2 + \varpi)^2} = \frac{(q^2 + \varpi)}{(p^2 + \varpi)} \leq 1. \quad (62)$$

Based on the matrix form of von Neumann analysis, we have proved that the numerical schemes are unconditionally stable.

3.4. Computational Procedure with Fixed Point Iteration

Here, the iterative procedure is carried out using the Gauss-Seidel (GS) iterative method (Kwok, 2011; Chapra, 2012). We first initialize $s_{f(m)}^n, (u_m)_i^n, (w_m)_i^n, (y_m)_i^n, (z_m)_i^n, (\Theta_m)_i^n$, and $(K_m)_i^n$ where $(u_l)_i^n, (w_l)_i^n, (y_l)_i^n$ and $(z_l)_i^n$ are calculated based on (49). We assume that $(u_m)_i^{n+1(lt=0)} = (u_m)_i^n, (w_m)_i^{n+1(lt=0)} = (w_m)_i^n, (y_m)_i^{n+1(lt=0)} = (y_m)_i^n$, and $(z_m)_i^{n+1(lt=0)} = (z_m)_i^n$ where "lt" is the iteration counter. $(u_l)_i^{n+1}, (w_l)_i^{n+1}, (y_l)_i^{n+1}$ and $(z_l)_i^{n+1}$ are calculated based on (49). Next, $(u_m)_i^{n+1(lt=1)}$ is computed and $s_{f(m)}^{n+1(lt=1)}$ is obtained from $(u_m)_0^{n+1(lt=1)}$. Subsequently, we compute $(w_m)_i^{n+1(lt=1)}, (y_m)_i^{n+1(lt=1)}, (z_m)_i^{n+1(lt=1)}, (\Theta_m)_i^{n+1(lt=1)}, (K_m)_i^{n+1(lt=1)}$, and $(\Gamma_m)_i^{n+1(lt=1)}$. The iterative process continues until the convergence criterion $\max_{1 \leq m \leq l} |s_{f(m)}^{n+1(lt+1)} - s_{f(m)}^{n+1(lt)}|, |(u_m)_i^{n+1(lt+1)} - (u_m)_i^{n+1(lt)}| < \varepsilon$ is satisfied. An algorithm for obtaining the numerical solutions of the optimal exercise boundary, asset option and the option Greeks in each regime using the GS method is described below.

Algorithm 1. Algorithm for the Proposed Method 1: Gauss-Seidel Iteration (FF-CS1 and FF-CS2)

Initialize $s_{f(m)}^n, (u_m)_i^n, (w_m)_i^n, (y_m)_i^n, (z_m)_i^n, (\Theta_m)_i^n, (K_m)_i^n,$ and $(\Gamma_m)_i^n$ for $i = 0, 1, \dots, M$ and $m = 1, 2, \dots, I$.

for n = 1 to N

Compute $(u_l)_i^n$ and $(w_l)_i^n, (y_l)_i^n$ and $(z_l)_i^n$ for $l = 1, 2, \dots, I$ and $l \neq m$ based on (49).

Set $s_{f(m)}^{n+1(lt=0)} = s_{f(m)}^n, (u_m)_i^{n+1(lt=0)} = (u_m)_i^n, (w_m)_i^{n+1(lt=0)} = (w_m)_i^n, (y_m)_i^{n+1(lt=0)} = (y_m)_i^n,$
 $(z_m)_i^{n+1(lt=0)} = (z_m)_i^n.$

while true

Compute $(u_l)_i^{n+1}, (w_l)_i^{n+1}, (y_l)_i^{n+1}$ and $(z_l)_i^{n+1}$ for $l = 1, 2, \dots, I$ and $l \neq m$ based on (49)

for m = 1 to I

Compute $(u_m)_i^{n+1(lt+1)}$ and evaluate $s_{f(m)}^{n+1(lt+1)}$ based on (42b), (44a) and (45a).

Evaluate $(w_m)_i^{n+1(lt+1)}$ based on (44b).

Evaluate $(y_m)_i^{n+1(lt+1)},$ and $(z_m)_i^{n+1(lt+1)}$ based on (44c) and (44d).

end

if $\max_{1 \leq m \leq I} |s_{f(m)}^{n+1(lt+1)} - s_{f(m)}^{n+1(lt)}| < \varepsilon$ and $\max_{1 \leq m \leq I} |(u_m)_i^{n+1(lt+1)} - (u_m)_i^{n+1(lt)}| < \varepsilon$

Calculate $(\Theta_m)_i^{n+1(lt+1)},$ and $(K_m)_i^{n+1(lt+1)},$ and $(\Gamma_m)_i^{n+1(lt+1)}$ based on (47) and (48).

Set $s_{f(m)}^n = s_{f(m)}^{n+1}, (u_m)_i^n = (u_m)_i^{n+1}, (w_m)_i^n = (w_m)_i^{n+1}, (y_m)_i^n = (y_m)_i^{n+1},$ and $(z_m)_i^n = (z_m)_i^{n+1(lt+1)}.$ *break;*

else

Set $s_{f(m)}^{n+1(lt)} = s_{f(m)}^{n+1(lt+1)}, (u_m)_i^{n+1(lt)} = (u_m)_i^{n+1(lt+1)}, (w_m)_i^{n+1(lt)} = (w_m)_i^{n+1(lt+1)}, (y_m)_i^{n+1(lt)} = (y_m)_i^{n+1(lt+1)},$ and $(z_m)_i^{n+1(lt)} = (z_m)_i^{n+1(lt+1)}.$

end

end

end

3.5. Computational Procedure with Newton Iterative Method

Newton method is known to provide quadratic convergence to the solution $F(\mathbf{x}) = 0$ and solving our numerical scheme with this method present an alternative and good choice. Based on (42) and (44), we start off our iteration in the form

$$F(\mathbf{u}_m^{n+1(lt=0)}) = A_m^u \mathbf{u}_m^{n+1(lt=0)} - (\mathbf{b}_m^u)^n; \quad F(\mathbf{w}_m^{n+1(lt=0)}) = A_m \mathbf{w}_m^{n+1(lt=0)} - (\mathbf{b}_m^w)^n; \quad (63a)$$

$$F(\mathbf{y}_m^{n+1(lt=0)}) = A_m \mathbf{y}_m^{n+1(lt=0)} - (\mathbf{b}_m^y)^n; \quad F(\mathbf{z}_m^{n+1(lt=0)}) = A_m \mathbf{z}_m^{n+1(lt=0)} - (\mathbf{b}_m^z)^n. \quad (63b)$$

Matrix A_m^u is symmetric, sparse and tridiagonal with constant coefficients likewise A_m . The former differs from the latter because of the boundary treatment in (42). Next, we evaluate

$$J_m^u(\mathbf{u}_m^{n+1(lt=0)}) \Delta \mathbf{u}_m^{n+1(lt=0)} = F(\mathbf{u}_m^{n+1(lt=0)}); J(\mathbf{w}_m^{n+1(lt=0)}) \Delta \mathbf{w}_m^{n+1(lt=0)} = F(\mathbf{w}_m^{n+1(lt=0)}); \quad (64a)$$

$$J(\mathbf{y}_m^{n+1(lt=0)}) \Delta \mathbf{y}_m^{n+1(lt=0)} = F(\mathbf{y}_m^{n+1(lt=0)}); J(\mathbf{z}_m^{n+1(lt=0)}) \Delta \mathbf{z}_m^{n+1(lt=0)} = F(\mathbf{z}_m^{n+1(lt=0)}). \quad (64b)$$

The advantage of our model is that the generated discrete Jacobian matrix is symmetric, sparse and tridiagonal with constant coefficients as one can easily observe from (42b) and (44). More precisely,

$$J_m^u(\mathbf{u}_m^n) \equiv A_m^u; J(\mathbf{w}_m^n) = J(\mathbf{y}_m^n) = J(\mathbf{z}_m^n) \equiv A_m \text{ for all } n \text{ where } m = 1, 2, \dots, I \quad (65)$$

It presents some nice properties that reduced the cost of computing the Jacobian matrix and enable the use of the Thomas Algorithm for solving $\Delta \mathbf{u}_m^{n+1(lt=0)}$, $\Delta \mathbf{w}_m^{n+1(lt=0)}$, $\Delta \mathbf{y}_m^{n+1(lt=0)}$, and $\Delta \mathbf{z}_m^{n+1(lt=0)}$. The next iteration is obtained as follows

$$\mathbf{u}_m^{n+1(lt=1)} = G(\mathbf{u}_m^{n+1(lt=0)}) = \mathbf{u}_m^{n+1(lt=0)} - \Delta \mathbf{u}_m^{n+1(lt=0)}; \quad (66a)$$

$$s_{f(m)}^{n+1(lt=1)} = K - (\mathbf{u}_m^{n+1(lt=1)})_{i=0}; \quad (66b)$$

$$\mathbf{w}_m^{n+1(lt=1)} = G(\mathbf{w}_m^{n+1(lt=0)}) = \mathbf{w}_m^{n+1(lt=0)} - \Delta \mathbf{w}_m^{n+1(lt=0)}; \quad (66c)$$

$$\mathbf{y}_m^{n+1(lt=1)} = G(\mathbf{y}_m^{n+1(lt=0)}) = \mathbf{y}_m^{n+1(lt=0)} - \Delta \mathbf{y}_m^{n+1(lt=0)}; \quad (66d)$$

$$\mathbf{z}_m^{n+1(lt=1)} = G(\mathbf{z}_m^{n+1(lt=0)}) = \mathbf{z}_m^{n+1(lt=0)} - \Delta \mathbf{z}_m^{n+1(lt=0)}. \text{ for } m = 1, 2, \dots, I. \quad (66e)$$

The iterative process continues until the convergence criterion $\max_{1 \leq m \leq I} |s_{f(m)}^{n+1(lt+1)} - s_{f(m)}^{n+1(lt)}|, |(\mathbf{u}_m)_i^{n+1(lt+1)} - (\mathbf{u}_m)_i^{n+1(lt)}| < \varepsilon$ is satisfied. It is important to further point out that to facilitate computation using Newton method, we adopt the procedure used in the work of Egorova et al (2016) and Khaliq and Liu by treating the coupled regime in the set of the system of PDE equations explicitly. An algorithm for obtaining the numerical solutions of the optimal exercise boundary, asset option and the option Greeks in each regime using the Newton method is described below.

Algorithm 2. Algorithm for the Proposed Method 2: Newton method (FF-CS3 and FF-CS4)

Initialize $s_{f(m)}^n, \mathbf{u}_m^n, \mathbf{w}_m^n, \mathbf{y}_m^n, \mathbf{z}_m^n, \Theta_m^n, \mathbf{K}_m^n$, and Γ_m^n for $m = 1, 2, \dots, I$.

for $n = 1$ **to** N

 Compute $\mathbf{u}_l^n, \mathbf{w}_l^n, \mathbf{y}_l^n, \mathbf{z}_l^n$ for $l = 1, 2, \dots, I$ and $l \neq m$ based on (49)

 Set $s_{f(m)}^{n+1(lt=0)} = s_{f(m)}^n, \mathbf{u}_m^{n+1(lt=0)} = \mathbf{u}_m^n, \mathbf{w}_m^{n+1(lt=0)} = \mathbf{w}_m^n, \mathbf{y}_m^{n+1(lt=0)} = \mathbf{y}_m^n, \mathbf{z}_m^{n+1(lt=0)} = \mathbf{z}_m^n$.

while true

```

for  $m = 1$  to  $I$ 
    Compute  $F(\mathbf{u}_m^{n+1(lt=0)})$ . Obtain  $\Delta \mathbf{u}_m^{n+1(lt=0)}$  using the Thomas Algorithm with  $J_m^u \equiv A_m^u$  based on (65). Compute  $\mathbf{u}_m^{n+1(lt=1)}$  based on (66) and evaluate  $S_{f(m)}^{n+1(lt=1)}$  from  $(\mathbf{u}_m^{n+1(lt=1)})_{i=0}$  based on (45).
end
if  $\max_{1 \leq m \leq I} |S_{f(m)}^{n+1(lt+1)} - S_{f(m)}^{n+1(lt)}| < \varepsilon$  and  $\max_{1 \leq m \leq I} |\mathbf{u}_m^{n+1(lt+1)} - \mathbf{u}_m^{n+1(lt)}| < \varepsilon$ 
    Calculate  $\Theta_m^{n+1}$  based on (47) and (48).
    Set  $S_{f(m)}^n = S_{f(m)}^{n+1}$ ,  $\mathbf{u}_m^n = \mathbf{u}_m^{n+1}$ 
    break;
else
    Set  $S_{f(m)}^{n+1(lt)} = S_{f(m)}^{n+1(lt+1)}$ ,  $\mathbf{u}_m^{n+1(lt)} = \mathbf{u}_m^{n+1(lt+1)}$ 
end
end
while true
    Compute  $\mathbf{w}_m^{n+1(lt+1)}$  in the same manner as  $\mathbf{u}_m^{n+1(lt+1)}$  based on (44), (65) and (66).
    Calculate  $\mathbf{K}_m^{n+1}$  based on (47) and (48).
end
while true
    Compute  $\mathbf{y}_m^{n+1(lt+1)}$  in the same manner as  $\mathbf{u}_m^{n+1(lt+1)}$  based on (44), (65) and (66).
    Calculate  $\mathbf{\Gamma}_m^{n+1}$  based on (47) and (48).
end
while true
    Compute  $\mathbf{z}_m^{n+1(lt+1)}$  in the same manner as  $\mathbf{u}_m^{n+1(lt+1)}$  based on (44), (65) and (66).
end
end

```

4. Numerical Experiment and Discussion

To test the accuracy and applicability of the present scheme, we present numerical examples, which are the American put options pricing problem with two regimes, four regimes, eight regimes, and sixteen regimes. The numerical code was written with MATLAB 2019a on Intel Core i5-3317U CPU 1.70GHz 64-bit ASUS Laptop. The numerical procedure was carried out on the mesh with a uniform grid size.

4.1. Numerical Examples: Two Regimes

We first considered the American put options with two regimes. We compared our present method labeled as

- a) Front Fixing-Compact Scheme with cubic Hermite interpolation and GS (FF-CS1)
- b) Front Fixing-Compact Scheme with quintic Hermite interpolation and GS (FF-CS2)
- c) Front Fixing-Compact Scheme with cubic Hermite interpolation and Newton Iteration (FF-CS3)
- d) Front Fixing-Compact Scheme with quintic Hermite interpolation and Newton Iteration (FF-CS4)

with MTree (Liu, 2010), IMS1, IMS2 (Khaliq and Liu, 2009), MOL (Chiarella et al, 2016), RBF-FD (Li et al, 2018), FF-expl (Egorova et al, 2016), ETD-CN (Khaliq et al, 2013), Iterated Optimal Stopping and Local Optimal Iteration (Babbin et al, 2011) as listed in Tables 1-5. The option Greeks results were also listed in Table 7.

Example 1: In our first example in this subsection, we consider a switching regime problem with the strike price chosen to be $K = 9$ at the expiration time $T = 1$. In our computation, we chose the interval $0 \leq x_m \leq 3$ with the grid size $h = 0.05$ and 0.01 for FF-CS1 and FF-CS2 and $h = 0.01$ for FF-CS3 and FF-CS4. The convergence criterion $\varepsilon = 10^{-8}$ was also chosen and the time step k was determined using $k = h^2$. The parameters are given as

$$Q = \begin{bmatrix} -6 & 6 \\ 9 & -9 \end{bmatrix}, \quad r = \begin{bmatrix} 0.10 \\ 0.05 \end{bmatrix}, \quad \sigma = \begin{bmatrix} 0.80 \\ 0.30 \end{bmatrix}. \quad (67)$$

Figs. 2 and 3 show the profile of the option prices, Greek parameters, and optimal exercise boundaries for the two-regimes case. From Tables 1-3, one can easily observe that the data obtained from FF-CS1 and FF-CS2, FF-CS3 and FF-CS4 when $h = 0.01$ is the same with the one obtained from MOL, MTree and RBF-FD up to 5 digits in most cases. However, FF-CS3 and FF-CS4 are more than five times faster than FF-CS1 and FF-CS2. Moreover, Chiarella et al (2016) pointed out that data obtained from MTree data was used as the benchmark in the work of Khaliq and Liu (2009). Generally, our data slightly decreases in direct proportion with h .

We choose not to use the derivative of the Hermite function to approximate $(y_l)_i^n$ and $(z_l)_i^n$. The reason is that the plots of the hedging parameters (beyond delta option) are more accurate and smoother if we approximate the coupled regime directly from the Hermite functions. In Fig. 5, we further investigate this effect by comparing the accuracy of our interpolated values and numerical results with built-in MATLAB cubic spline function. One can easily observe that the plot of gamma and speed options generated directly from

Hermite function are more accurate. However, it is important to point out that using the built-in-MATLAB spline function increases the average CPU time in each time step as shown in Table 6.

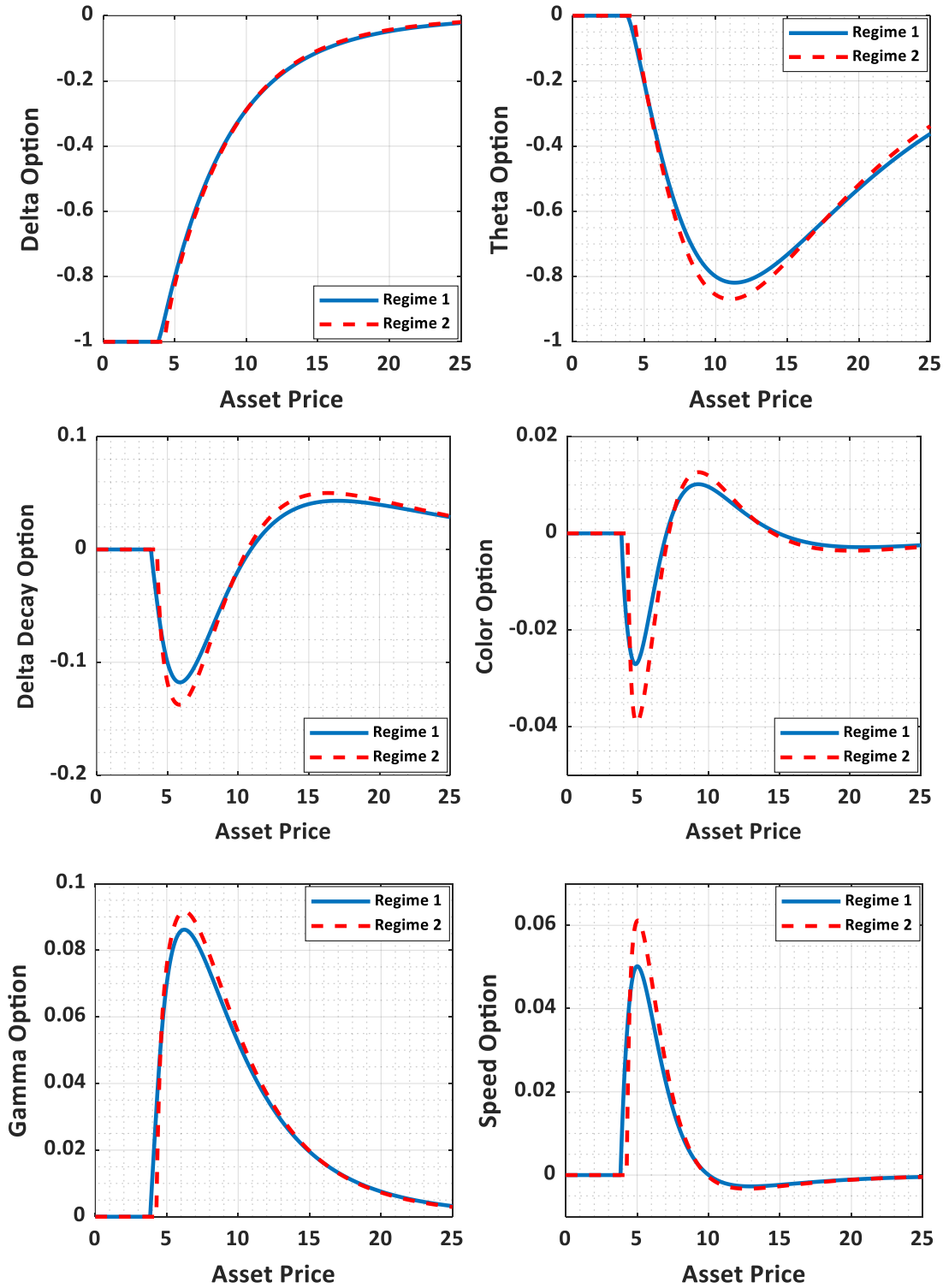


Fig. 2. Option Greeks for the two regimes case when $\tau = T$ (example 1).

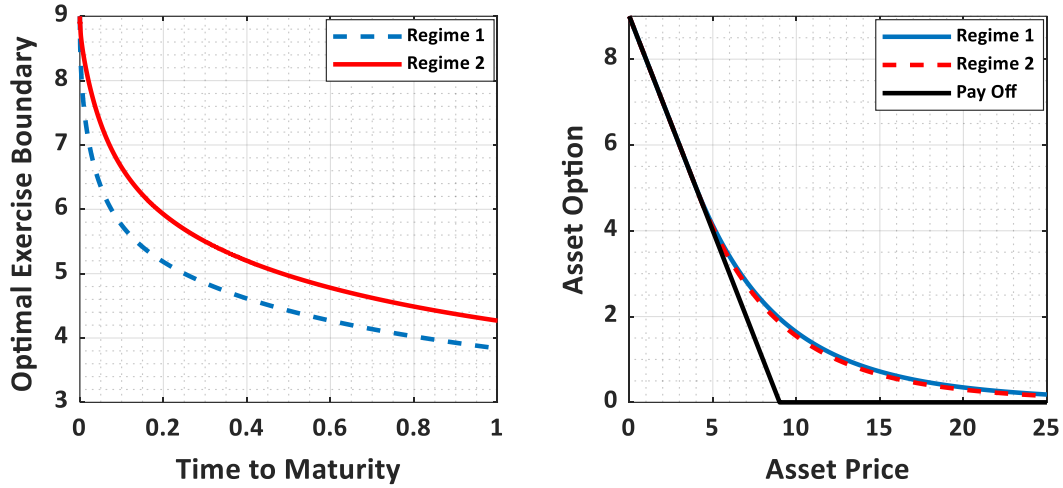


Fig. 3. Asset options and optimal exercise boundaries for the two regime case when $\tau = T$ (example 1).

Example 2: In the second example, we investigate the performance of our method with MOL when there is no jump between regimes (Chiarella et al, 2016; Meyer and van der Hoek, 1997). We use the same data provided in the first example. The grid size and generator matrix was chosen to be $h = 0.01$ and

$$Q = \begin{bmatrix} 0 & 0 \\ 0 & 0 \end{bmatrix}, \quad (68)$$

respectively. The obtained result is presented in Table 5. It is easy to see from Table 5 that the data from FF-CS1 and FF-CS2 are the same. This is because there was no jump between different states.

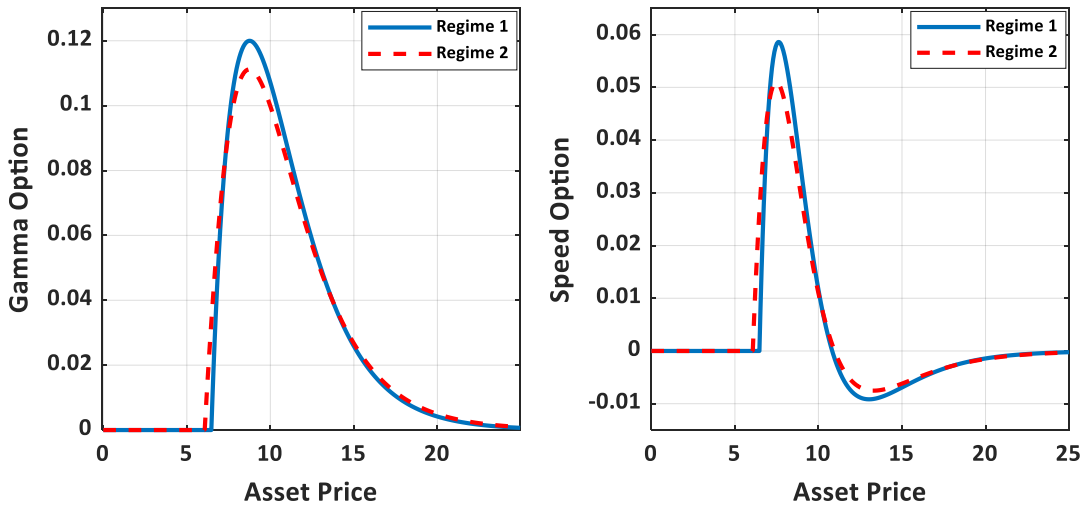


Fig. 4. Gamma and speed options for the two regime case when $\tau = T$ (example 3).

Example 3: Finally, we compared our results with Iterated Optimal Stopping and Local Optimal Iteration (Babbin et al, 2011). The strike price was chosen to be $K = 10$ at the expiration time $T = 1$. The grid size was chosen to be $h = 0.01$. The parameters are given as

$$Q = \begin{bmatrix} -3 & 3 \\ 2 & -2 \end{bmatrix}, \quad r = \begin{bmatrix} 0.05 \\ 0.05 \end{bmatrix}, \quad \sigma = \begin{bmatrix} 0.3 \\ 0.4 \end{bmatrix}. \quad (69)$$

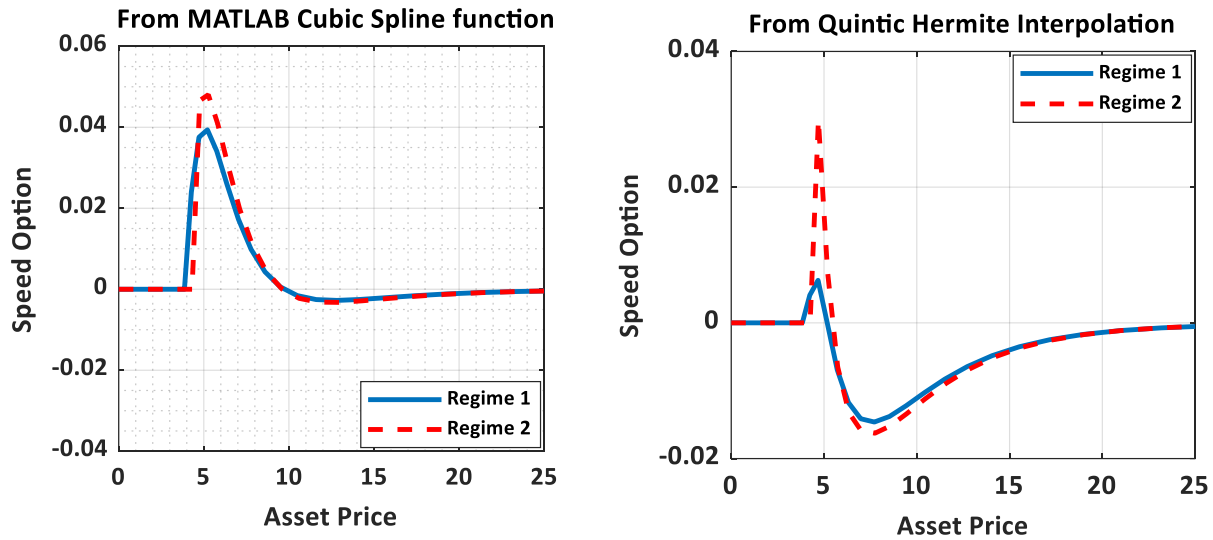


Fig. 5a. Comparing the plots of speed options generated from built-in-MATLAB cubic spline function and FF-CS2 when approximated from the derivative of the Hermite function for $h = 0.1$ (example 1).

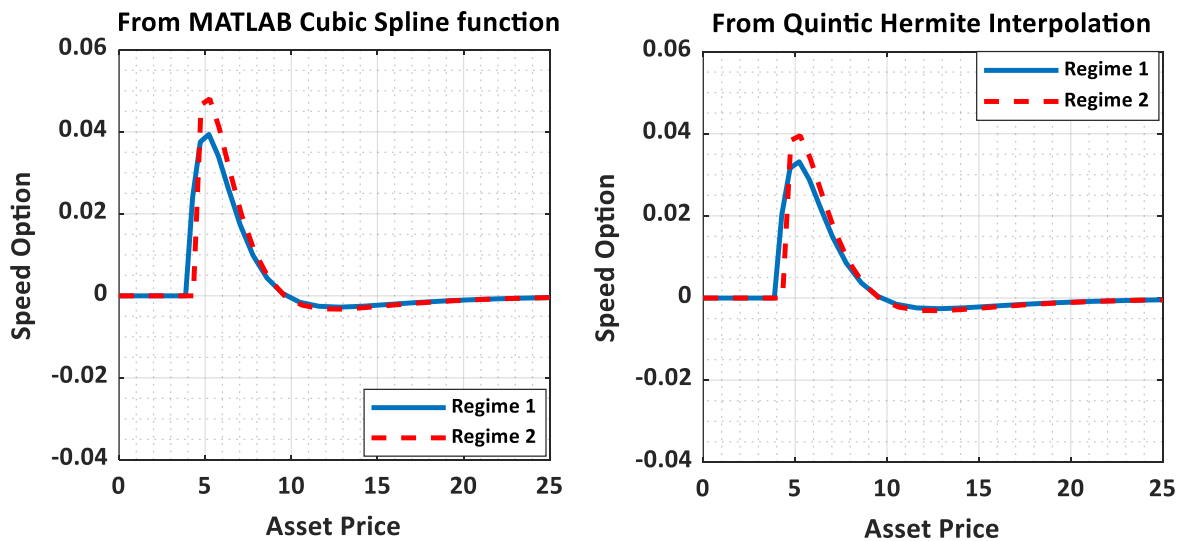


Fig. 5b. Comparing the plots of speed options generated from built-in-MATLAB cubic spline function and FF-CS2 when approximated directly from the Hermite function for $h = 0.1$ (example 1).

Table 1. Comparison of American put option price in regime 1 for example 1.

S	MTree	IMS1	IMS2	MOL	FF-CS1			FF-CS2		FF-CS3		FF-CS4
					$h = 0.1$	0.05	0.01	0.1	0.05	0.01	0.01	0.01
3.5	5.5000	5.5001	5.5001	5.5000	5.5000	5.5000	5.5000	5.5000	5.5000	5.0000	5.5000	5.0000
4.0	5.0066	5.0067	5.0066	5.0033	5.0068	5.0035	5.0033	5.5069	5.0035	5.0033	5.0033	5.0033
4.5	4.5432	4.5486	4.5482	4.5433	4.5475	4.5442	4.5433	4.5475	4.5442	4.5433	4.5433	4.5433
6.0	3.4144	3.4198	3.4184	3.4143	3.4189	3.4142	3.4143	3.4190	3.4143	3.4143	3.4141	3.4141
7.5	2.5844	2.5877	2.5867	2.5842	2.5873	2.5854	2.5842	2.5874	2.5854	2.5842	2.5840	2.5840
8.5	2.1560	2.1598	2.1574	2.1559	2.1539	2.1553	2.1559	2.1540	2.1553	2.1559	2.1556	2.1556
9.0	1.9722	1.9756	1.9731	1.9720	1.9759	1.9722	1.9720	1.9760	1.9723	1.9720	1.9717	1.9717
9.5	1.8058	1.8090	1.8064	1.8056	1.8043	1.8062	1.8056	1.8044	1.8062	1.8056	1.8054	1.8054
10.5	1.5186	1.5214	1.5187	1.5185	1.5170	1.5190	1.5185	1.5170	1.5190	1.5185	1.5183	1.5183
12.0	1.1803	1.1827	1.1799	1.1803	1.1833	1.1802	1.1803	1.1833	1.1802	1.1803	1.1801	1.1801

Table 2. Comparison of American put option price in regime 2 for example 1.

S	MTree	IMS1	IMS2	MOL	FF-CS1			FF-CS2		FF-CS3		FF-CS4
					$h = 0.1$	0.05	0.01	0.1	0.05	0.01	0.01	0.01
3.5	5.5000	5.5012	5.5012	5.5000	5.5000	5.5000	5.5000	5.5000	5.5000	5.5000	5.5000	5.5000
4.0	5.0000	5.0016	5.0016	5.0000	5.0000	5.0000	5.0000	5.0000	5.0000	5.0000	5.0000	5.0000
4.5	4.5117	4.5194	4.5190	4.5119	4.5183	4.5129	4.5119	4.5184	4.5129	4.5119	4.5119	4.5119
6.0	3.3503	3.3565	3.3550	3.3507	3.3552	3.3508	3.3507	3.3553	3.3508	3.3507	3.3504	3.3504
7.5	2.5028	2.5078	2.5056	2.5033	2.5070	2.5044	2.5033	2.5071	2.5045	2.5033	2.5030	2.5030
8.5	2.0678	2.0722	2.0695	2.0683	2.0677	2.0683	2.0683	2.0679	2.0684	2.0683	2.0681	2.0681
9.0	1.8819	1.8860	1.8832	1.8825	1.8864	1.8822	1.8825	1.8864	1.8820	1.8825	1.8822	1.8822
9.5	1.7143	1.7181	1.7153	1.7149	1.7116	1.7149	1.7149	1.7116	1.7149	1.7149	1.7146	1.7146
10.5	1.4267	1.4301	1.4272	1.4273	1.4240	1.4273	1.4273	1.4239	1.4274	1.4273	1.4271	1.4271
12.0	1.0916	1.0945	1.0916	1.0923	1.0948	1.0927	1.0923	1.0948	1.0927	1.0923	1.0921	1.0921

Table 3. Further Comparison of American put option price for example 1

S	RBF-FD		ETD-CN		FF-expl		FF-CS2 ($h = 0.01$)	
	Regime 1	Regime 2	Regime 1	Regime 2	Regime 1	Regime 2	Regime 1	Regime 2
6.0	3.4143	3.3507	3.4196	3.3563	~	~	3.4143	3.3507
7.5	2.5842	2.5033	2.5886	2.5077	~	~	2.5854	2.5033
9.0	1.9718	1.8825	1.9756	1.8859	1.9713	1.8817	1.9720	1.8825
9.5	~	~	1.8089	1.7181	1.8049	1.7141	1.8056	1.7149
10.5	1.5185	1.4274	1.5213	1.4301	1.5177	1.4265	1.5185	1.4273
12.0	1.1803	1.0924	1.1825	1.0945	1.1796	1.0915	1.1803	1.0923

Table 4. Comparing FF-CS3, and FF-CS4 up to sixteen digit at strike price in example 1

Strike price	FF-CS3		FF-CS4	
	Regime 1	Regime 2	Regime 1	Regime 2
9.0	1.971738757801249	1.882203676543793	1.971733636374602	1.882198321043946

Table 5. Comparison of American put option price with no jump between regimes for example 2.

S	MOL	FF-CS1	FF-CS2
---	-----	--------	--------

	Regime 1	Regime 2	Regime 1	Regime 2	Regime 1	Regime 2
6.00	3.666762424	3.000000000	3.666746420	3.000000000	3.666746420	3.000000000
9.00	2.375385605	0.888311178	2.375408073	0.888393716	2.375408073	0.888393716
12.00	1.604853957	0.203543056	1.604912489	0.204583983	1.604912489	0.203637945

Table 6. Comparison of American put option price with IOS and LOI in Regime 1 for example 3.

S	IOS	LOI	RBF-FD	FF-CS2	FF-CS4
Maximum Refinement				$h = 0.01$	
10.00	1.174796138	1.1747960	1.1756722	1.1750372	1.1751356

Table 7. American put option Greeks for the two regimes in example 1 with FF-CS4

S	Delta		Gamma		Speed		Theta		Delta-Decay		Color	
	Reg 1	Reg 2	Reg 1	Reg 2	Reg 1	Reg 2	Reg 1	Reg 2	Reg 1	Reg 2	Reg 1	Reg 2
3.5	-1.0000	-1.0000	0.0000	0.0000	0.0000	0.0000	0.0000	0.0000	0.0000	0.0000	0.0000	0.0000
4.0	-0.9653	-1.0000	0.0165	0.0000	0.0171	0.0000	-0.0299	0.0000	-0.0211	0.0000	-0.0086	0.0000
4.5	-0.8750	-0.9173	0.0510	0.0499	0.0439	0.0471	-0.1199	-0.0848	-0.0692	-0.0723	-0.0228	-0.0295
6.0	-0.6426	-0.6571	0.0854	0.0909	0.0382	0.0463	-0.4081	-0.4277	-0.1164	-0.1362	-0.0123	-0.0205
9.5	-0.3165	-0.3181	0.0562	0.0596	0.0015	0.0013	-0.7900	-0.8463	-0.0313	-0.0320	0.0109	0.0133
12.0	-0.1945	-0.1913	0.0348	0.0362	-0.0025	-0.0031	-0.8244	-0.8696	0.0167	0.0238	0.0061	0.0069

Like other given examples, the convergence criterion $\varepsilon = 10^{-8}$ was chosen and the time step k was determined using $k = h^2$. In Table 6, we compare the result with RBF-FD, IOS, and LOP methods. The gamma and speed plots from this example are shown in Fig. 4.

To check the accuracy of our present method, we calculated the convergence rate from the asset option in regime 1. To obtain the convergence rate of our numerical scheme, we defined the maximum error using the notation

$$E(h, k) = \max_{0 \leq i \leq M} |(u_1)_i^n(h, k) - (u_1)_i^n(h/2, k/4)| \quad (70)$$

$$E(h/2, k/4) = \max_{0 \leq i \leq M} |(u_1)_i^n(h/2, k/4) - (u_1)_i^n(h/4, k/16)| \quad (71)$$

Table 8. The maximum errors and convergent rates for regime 1 in example 1.

h	k	convergent rate	
		FF-CS1	FF-CS2
2×10^{-1}	4×10^{-2}		
1×10^{-1}	1×10^{-2}		
5×10^{-2}	2.5×10^{-3}	3.43	3.27
2.5×10^{-2}	6.25×10^{-4}	3.82	3.78
1.25×10^{-2}	1.5625×10^{-4}	3.67	3.98

where $k = h^2$. $(u_1)_i^n(h, k)$, $(u_1)_i^n(h/2, k/4)$, and $(u_1)_i^n(h/4, k/16)$, are the numerical solution from regime 1 obtained based on h and k , $h/2$ and $k/4$, and $h/4$ and $k/16$, respectively. As such, the convergence rate can be evaluated using the equation in (72) as shown in Table 8.

$$\text{Rate} = \log_2 \frac{E(h, k)}{E(h/2, k/4)}. \quad (72)$$

Table 9. Average CPU time(s) per each time step for the two-regimes example

h	CPU Time(s)					
	Built-in MATLAB Spline Function		FF-CS1	FF-CS2	FF-CS3	FF-CS4
	GS iteration	Newton Iteration				
0.1	19.39	0.302	0.182	0.209	0.058	0.061
0.05	105.6	0.455	0.311	0.316	0.084	0.078
0.01	204.6	3.291	3.697	4.167	0.768	0.771

Table 8 lists the maximum errors and convergence rates based on $h = 0.2, 0.1, 0.05, 0.025, 0.0125$, respectively. From Table 8, we see that the convergence rate in space is round about 3.75 and 3.85 for FF-CS1 and 3.85, respectively. In general, the computation speed of FF-CS1, FF-CS2, FF-CS3, and FF-CS4 is very fast and the average CPU time at each time step is shown in Table 9.

4.2. Numerical Examples beyond Two Regimes

Commonly, previous works of literature have limited the regime-switching analysis to two and four regimes. Moreover, Chiarella et al. (2016) and Khaliq and Liu (2008) pointed out that the method proposed by Buffington and Elliot (2002) cannot be extended beyond two regimes. To show that our method can compute a large finite state space, we wrote a sequence of MATLAB function files and used it to write a few lines of code that can take any number of finite state space. We then considered the American put options pricing problem with four, eight, and sixteen regimes. The strike price and expiration time were chosen to be $K = 9$ and $T = 1$, respectively. In our computation, we chose the interval $0 \leq x_m \leq 3$ where the grid size $h = 10^{-2}$ and $k = 10^{-4}$. The convergence criterion $\varepsilon = 10^{-7}$ was also chosen for the four regimes and the latter was computed with FF-CS2. For the eight and sixteen regimes, the convergence criterion $\varepsilon = 10^{-8}$ was chosen and was computed with FF-CS3.

Four-regimes example:

$$Q = \begin{bmatrix} -1 & 1/3 & 1/3 & 1/3 \\ 1/3 & -1 & 1/3 & 1/3 \\ 1/3 & 1/3 & -1 & 1/3 \\ 1/3 & 1/3 & 1/3 & -1 \end{bmatrix}, \quad r = \begin{bmatrix} 0.02 \\ 0.10 \\ 0.06 \\ 0.15 \end{bmatrix}, \quad \sigma = \begin{bmatrix} 0.90 \\ 0.50 \\ 0.70 \\ 0.20 \end{bmatrix}. \quad (73)$$

Eight-regimes example:

$$Q = \begin{bmatrix} -1 & 0.2 & 0.2 & 0.2 & 0.1 & 0.1 & 0.1 & 0.1 \\ 0.2 & -1 & 0.1 & 0.1 & 0.1 & 0.2 & 0.2 & 0.1 \\ 0.2 & 0.1 & -1 & 0.1 & 0.2 & 0.1 & 0.1 & 0.2 \\ 0.2 & 0.1 & 0.2 & -1 & 0.2 & 0.1 & 0.1 & 0.1 \\ 0.1 & 0.2 & 0.1 & 0.1 & -1 & 0.2 & 0.1 & 0.2 \\ 0.2 & 0.2 & 0.2 & 0.1 & 0.1 & -1 & 0.1 & 0.1 \\ 0.1 & 0.1 & 0.2 & 0.2 & 0.2 & 0.1 & -1 & 0.1 \\ 0.1 & 0.1 & 0.1 & 0.2 & 0.1 & 0.2 & 0.2 & -1 \end{bmatrix}, \quad r = \begin{bmatrix} 0.03 \\ 0.15 \\ 0.20 \\ 0.09 \\ 0.05 \\ 0.12 \\ 0.15 \\ 0.18 \end{bmatrix}, \quad \sigma = \begin{bmatrix} 0.80 \\ 0.40 \\ 0.50 \\ 0.70 \\ 0.45 \\ 0.38 \\ 0.30 \\ 0.25 \end{bmatrix}. \quad (74)$$

Sixteen-regimes example:

$$r = [0.04 \ 0.15 \ 0.03 \ 0.30 \ 0.13 \ 0.12 \ 0.10 \ 0.18 \ 0.08 \ 0.25 \ 0.06 \ 0.20 \ 0.21 \ 0.07 \ 0.12 \ 0.19],$$

$$\sigma = [0.07 \ 0.30 \ 0.90 \ 0.80 \ 0.25 \ 0.15 \ 0.12 \ 0.28 \ 0.85 \ 0.35 \ 0.39 \ 0.72 \ 0.45 \ 0.18 \ 0.20 \ 0.25].$$

$$Q = \begin{bmatrix} -3 & 0.2 & 0.2 & 0.2 & 0.2 & \cdots & 0.2 & 0.2 & 0.2 & 0.2 & 0.2 \\ 0.2 & -3 & 0.2 & 0.2 & 0.2 & \cdots & 0.2 & 0.2 & 0.2 & 0.2 & 0.2 \\ 0.2 & 0.2 & -3 & 0.2 & 0.2 & \cdots & 0.2 & 0.2 & 0.2 & 0.2 & 0.2 \\ 0.2 & 0.2 & 0.2 & -3 & 0.2 & \cdots & 0.2 & 0.2 & 0.2 & 0.2 & 0.2 \\ 0.2 & 0.2 & 0.2 & 0.2 & -3 & \cdots & 0.2 & 0.2 & 0.2 & 0.2 & 0.2 \\ \vdots & \vdots & \vdots & \vdots & \vdots & \ddots & \vdots & \vdots & \vdots & \vdots & \vdots \\ 0.2 & 0.2 & 0.2 & 0.2 & 0.2 & \cdots & 0.2 & -3 & 0.2 & 0.2 & 0.2 \\ 0.2 & 0.2 & 0.2 & 0.2 & 0.2 & \cdots & 0.2 & 0.2 & -3 & 0.2 & 0.2 \\ 0.2 & 0.2 & 0.2 & 0.2 & 0.2 & \cdots & 0.2 & 0.2 & 0.2 & -3 & 0.2 \\ 0.2 & 0.2 & 0.2 & 0.2 & 0.2 & \cdots & 0.2 & 0.2 & 0.2 & 0.2 & -3 \end{bmatrix}, \quad (75)$$

Figs. 6-9 plot the profiles of the option prices, Greek parameters, and optimal exercise boundaries for the four, eight, and sixteen regimes. Table 10-12 lists the option prices and Greeks of the four, eight and sixteen regimes using the asset values in the interval of $3.5 \leq S \leq 12$.

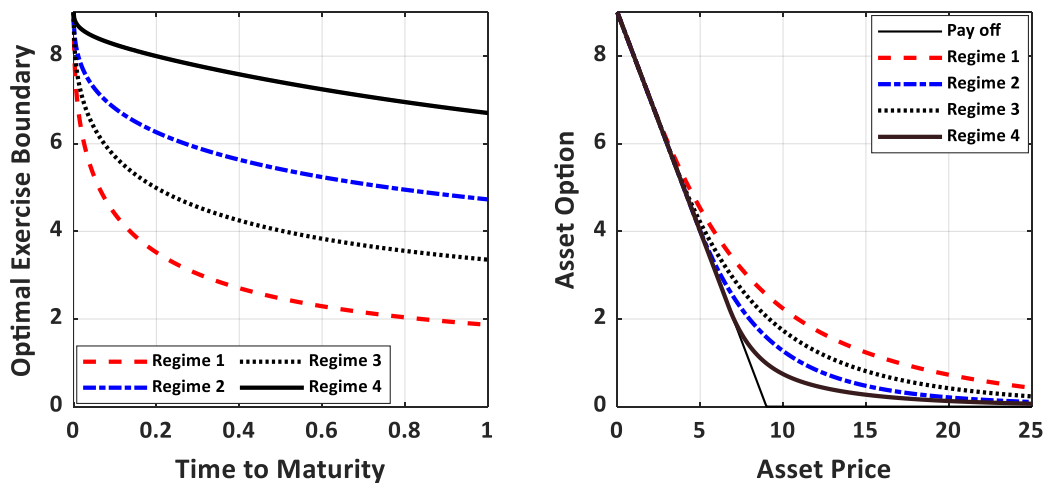


Fig. 6. Asset options and optimal exercise boundaries for the four regime case when $\tau = T$.

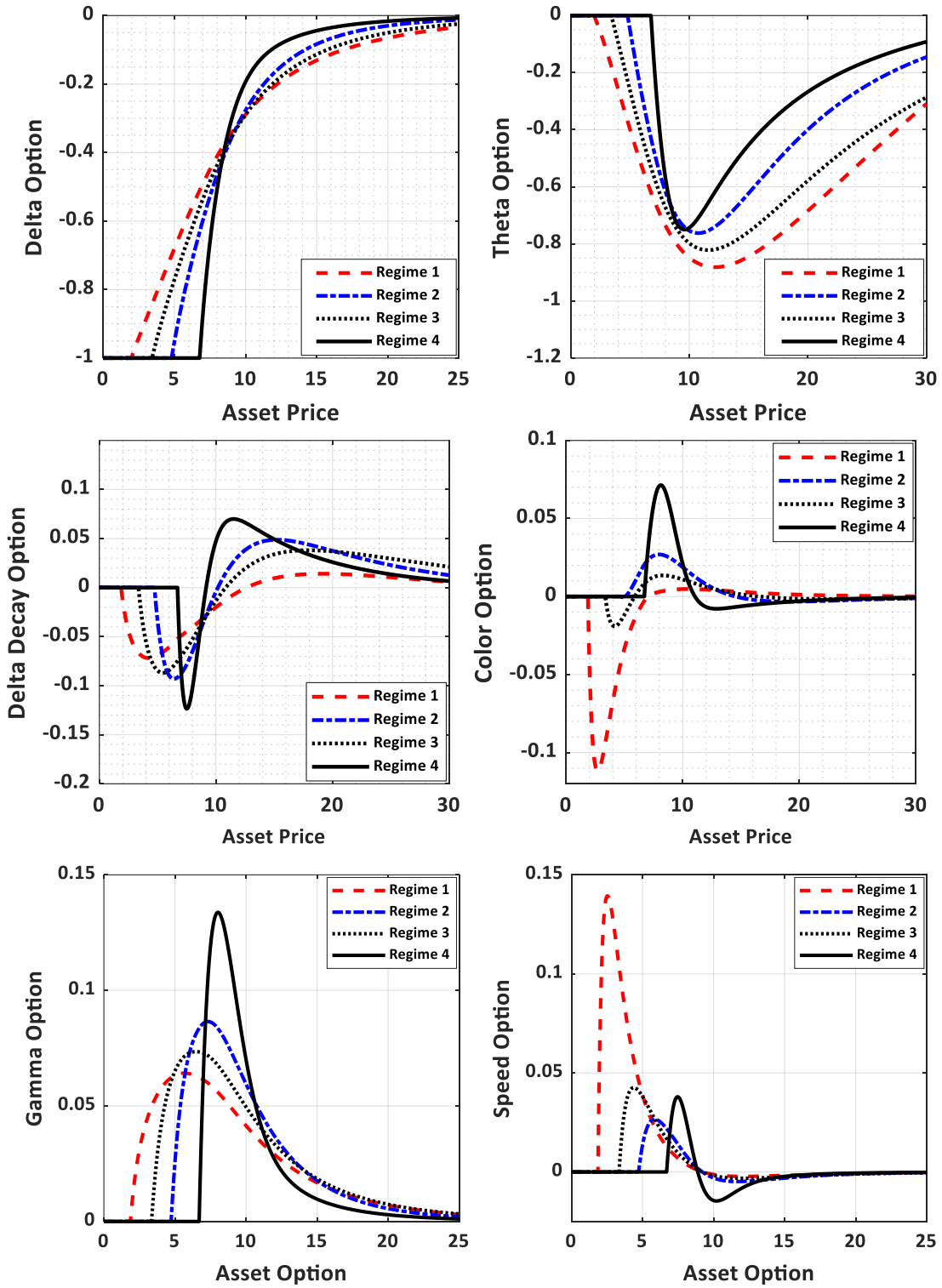


Fig. 7. Option Greeks for the four regime case when $\tau = T$.

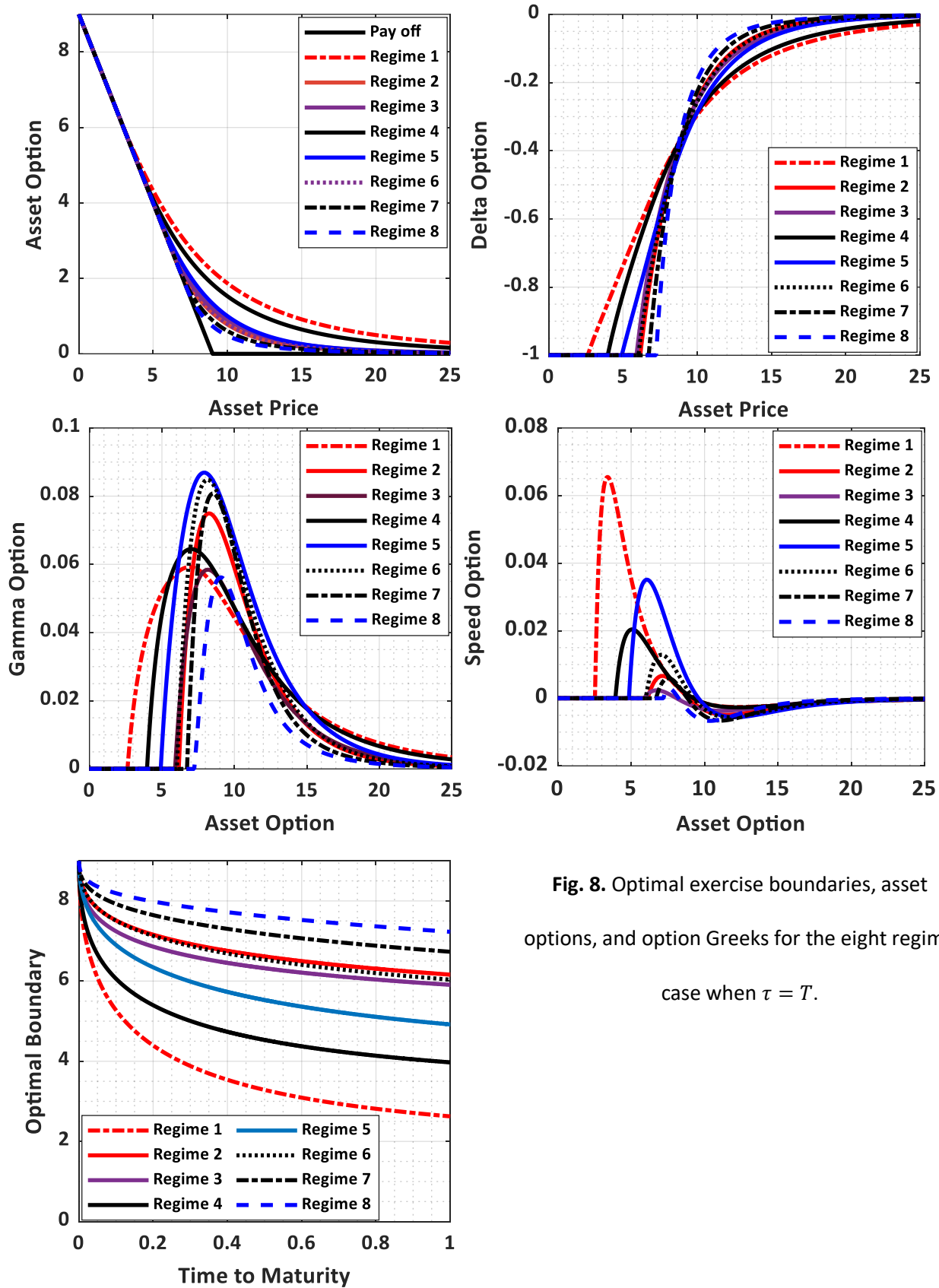
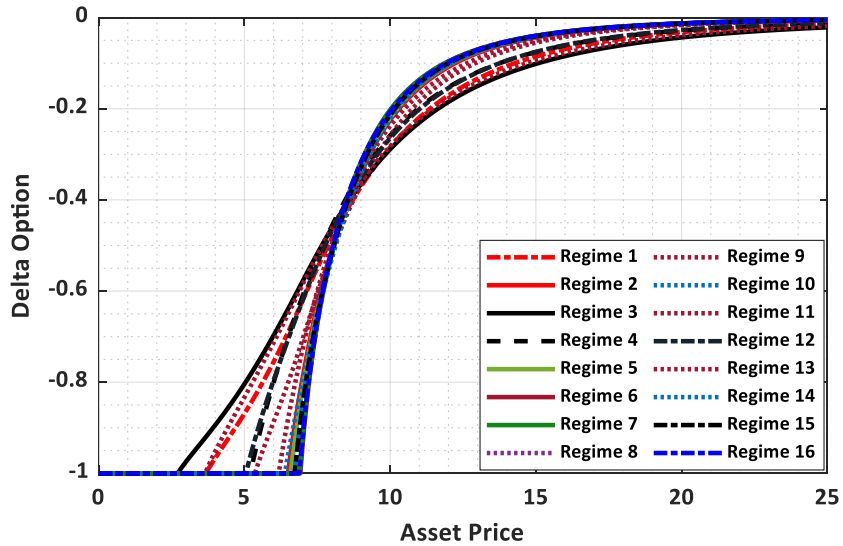
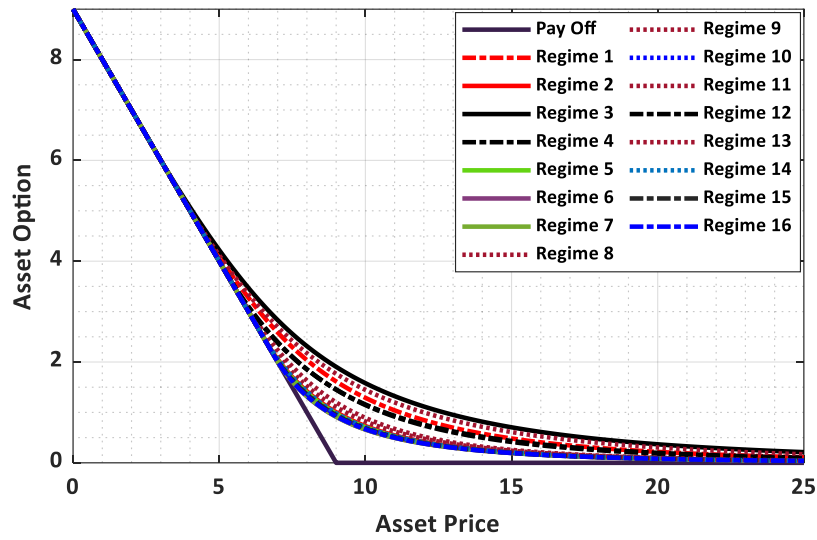
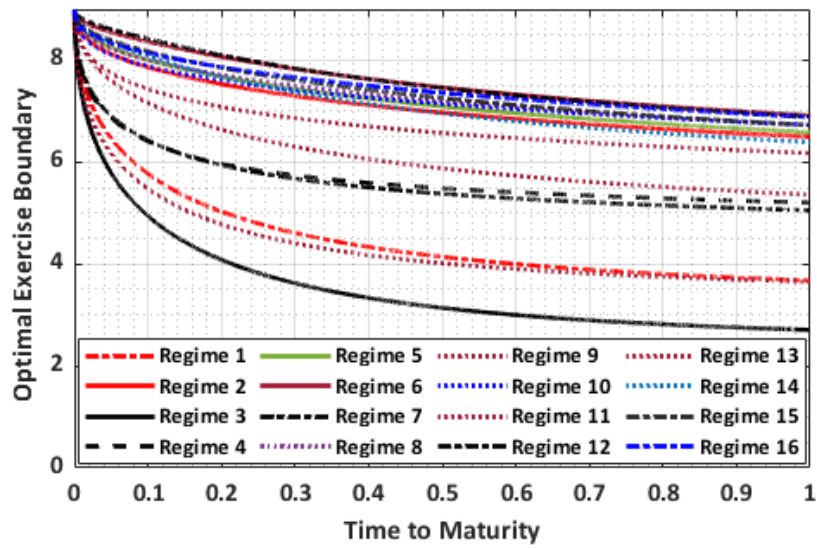


Fig. 8. Optimal exercise boundaries, asset options, and option Greeks for the eight regime case when $\tau = T$.



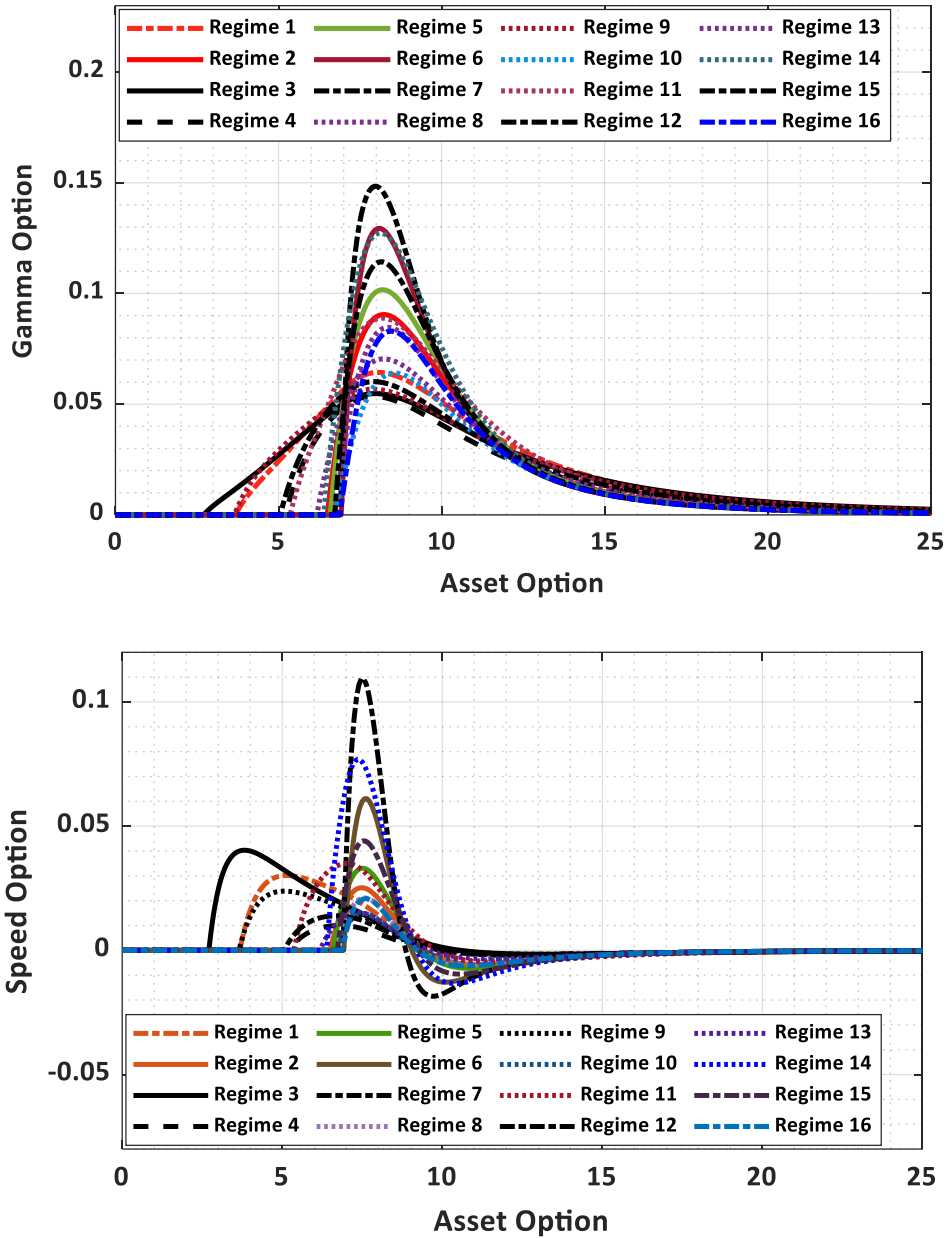


Fig. 9. Optimal exercise boundaries, asset options, and option Greeks for the sixteen regime case when $\tau = T$.

At the money option, volatility has a negligible impact on the delta option for all the regimes. Hence, the plot for each regime intersects at the strike price. For long put options, as we move deep in the money and out of the money, delta converges to -1 and 0, respectively. Gamma is maximum when at the money. Ignoring the sign convention, the theta of ATM is maximum. Delta decay and color options measure the rate at which delta and gamma options decay respectively.

Table 10. Comparison of American put options price for the four regimes' example with FF-CS2

S	MTree				RBF-FD				FF-expl			
	Reg 1	Reg 2	Reg 3	Reg 4	Reg 1	Reg 2	Reg 3	Reg 4	Reg 1	Reg 2	Reg 3	Reg 4
7.5	3.1433	2.2319	2.6746	1.6574	3.1424	2.2320	2.6744	1.6576	3.1421	2.2313	2.6739	1.6573
9.0	2.5576	1.5834	2.0568	0.9855	2.5564	1.5835	2.0566	0.9857	2.5563	1.5827	2.0559	0.9850
10.5	2.1064	1.1417	1.6014	0.6533	2.1052	1.1415	1.6013	0.6554	2.1047	1.1406	1.6004	0.6546
12.0	1.7545	0.8377	1.2625	0.4708	1.7527	0.8377	1.2625	0.4708	1.7524	0.8368	1.2614	0.4700
S	ETD-CN				MOL				FF-CS2			
	Reg 1	Reg 2	Reg 3	Reg 4	Reg 1	Reg 2	Reg 3	Reg 4	Reg 1	Reg 2	Reg 3	Reg 4
7.5	3.1513	2.2384	2.6813	1.6664	3.1432	~	~	~	3.1414	2.2319	2.6745	1.6577
9.0	2.5641	1.5884	2.0623	0.9903	2.5576	~	~	~	2.5545	1.5834	2.0567	0.9858
10.5	2.1113	1.1451	1.6057	0.6580	2.1063	~	~	~	2.1012	1.1413	1.6012	0.6553
12.0	1.7578	0.8377	1.2658	0.4725	1.7544	~	~	~	1.7465	0.8374	1.2621	0.4706

Table 11. American Put Option Greeks for the four regimes' example with FF-CS1

S	Delta				Gamma				Speed			
	Reg 1	Reg 2	Reg 3	Reg 4	Reg 1	Reg 2	Reg 3	Reg 4	Reg 1	Reg 2	Reg 4	
3.5	-0.8246	-1.0000	-0.9744	-1.0000	0.0515	0.0000	0.0122	0.0000	0.0949	0.0000	0.0000	
6.0	-0.5739	-0.7442	-0.6392	-1.0000	0.0638	0.0723	0.0727	0.0000	0.0204	0.0262	0.0000	
9.0	-0.3401	-0.3546	-0.3520	-0.3026	0.0488	0.0727	0.0589	0.1086	5.2790e-04	0.0011	-0.0027	
12.0	-0.2055	-0.1679	-0.1953	-0.0958	0.0289	0.0370	0.0335	0.0269	-0.0023	-0.0048	-0.0081	

Table 12. American put options price for the eight, and sixteen regimes' example with FF-CS4

S	Eight regimes					Sixteen regimes						
	Reg 1	Reg 2	Reg 4	Reg 6	Reg 8	Reg 1	Reg 2	Reg 4	Reg 6	Reg 8	Reg 12	Reg 16
3.5	5.5555	5.5000	5.5000	5.5000	5.5000	5.5000	5.5000	5.5000	5.5000	5.5000	5.5000	5.5000
4.0	5.1244	5.0000	5.0006	5.0000	5.0000	5.0075	5.0000	5.0000	5.0000	5.0000	5.0000	5.0000
4.5	4.7197	4.5000	4.5320	4.5000	4.5000	4.5387	4.5000	4.5000	4.5000	4.5000	4.5000	4.5000
6.0	3.6639	3.0000	3.3649	3.0001	3.0000	3.2836	3.0000	3.0872	3.0000	3.0000	3.1064	3.0000
7.5	2.8408	1.7962	2.4959	1.8252	1.5301	2.3078	1.7145	2.1059	1.6227	1.6611	2.1163	1.6249
8.5	2.4081	1.2864	2.0536	1.3138	0.9338	1.8264	1.2061	1.6496	1.1089	1.1555	1.6497	1.1146
9.0	2.2214	1.0921	1.8662	1.1169	0.7457	1.6290	1.0209	1.4662	0.9312	0.9767	1.4619	0.9379
9.5	2.0519	0.9293	1.6985	0.9510	0.6033	1.4563	0.8697	1.3072	0.7900	0.8319	1.2992	0.7964
10.5	1.7582	0.6785	1.4129	0.6945	0.4094	1.1721	0.6435	1.0484	0.5884	0.6114	1.0347	0.5885
12.0	1.4092	0.4334	1.0838	0.4428	0.2482	0.8617	0.4286	0.7692	0.3929	0.4081	0.7509	0.3938

5. Conclusion

We have developed an accurate numerical method for solving American put options with regime-switching. Through the front-fixing transformations, we were able to fix the optimal exercise boundary for each regime. The derivative transformation enables us to employ the fourth-order compact finite difference method coupled with the high order interpolation technique for solving the system of the asset,

delta, gamma, and speed options while capturing the optimal exercise boundary and theta, delta decay and color options. Moreover, our method has a substantial advantage because it simultaneously and accurately calculates asset, delta, gamma, speed, theta, delta decay and color options, and optimal exercise boundary during iteration. Greek parameters are difficult to estimate correctly as can be seen from previous works of literature. However, by formulating a set of a system of PDEs that consist of the asset option and its derivatives for each regime, we were able to estimate those parameters with high-order accuracy. Our method and numerical discretization also present a sparse, symmetric, tridiagonal, positive definite and constant co-efficient and Jacobian matrix which enables us to implement both fixed point and Newton iteration (with Thomas algorithm) with ease and less computation. The present scheme has been tested in two, four, eight, and sixteen regimes problems and with cubic and quintic Hermite and cubic spline interpolation. The results show that the method provides an accurate solution and fast in computation as compared with the existing methods. The future research will include applying this method to non-constant volatility and/or interest rate.

References

1. Adam, Y. (1975). A Hermitian finite difference method for the solution of parabolic equation. *Computers and Mathematics with Applications*, 1, 393-406.
2. Babbin, J. Forsyth, P. A., and Labahn, G. (2014). A comparison of iterated optimal stopping and local policy iteration for American options under regime switching. *J. Sci. Comput.* 58, 409–430.
3. Bidégaray-Fesquet, B. (2006). Von-Neumann stability analysis of FD-TD methods in complex media.
4. Bingham, N. H. (2006). Financial modeling with jump processes. *Journal of the American Statistical Association*, 101 (475), 1315–1316 (<https://doi:10.1198/jasa.2006.s130>).
5. Blackwell, B. F., and Hogan, R. E. (1994). One-dimensional ablation using Landau transformation and finite control volume procedure. *Journal of Thermophysics and Heat Transfer*, 8 (2), 282–287 (<https://doi:10.2514/3.535>).
6. Boyarchenko, S. I., and Levendorskii, S. Z. (2008). Pricing American options in regime-switching models: FFT Realization. *SSRN Electronic Journal* (<https://doi:10.2139/ssrn.1127562>).
7. Buffington, J., and Elliott, R. J. (2002). American options with regime-switching. *International Journal of Theoretical and Applied Finance*, 05 (05), 497–514 (<https://doi:10.1142/s0219024902001523>).

8. Burden, R. L., Faires, D. J., and Burden, A. M. (2016). Numerical analysis. Cengage Learning, Boston, MA.
9. Cao, H. H., Liu, L. B., Zhang, Y., and Fu, S. M. (2011). A fourth-order method of the convection-diffusion equation with Neumann boundary conditions. *Applied Mathematics and Computation*, 217 (2011) 9133-9141.
10. Chapra, S. C. (2012). Applied numerical methods with MATLAB for engineers and scientist. MC Graw-Hill, New York.
11. Chen, Y., Xiao, A., and Wang, W. (2019). An IMEX-BDF2 compact scheme for pricing options under regime-switching jump-diffusion models. *Mathematical Methods in the Applied Sciences*, (<https://doi:10.1002/mma.5539>).
12. Chiarella, C., Nikitopoulos Sklibosios, C., Schlogl, E., and Yang, H. (2016). Pricing American options under regime switching using method of lines. *SSRN Electronic Journal*, (<https://doi:10.2139/ssrn.2731087>).
13. Chockalingam, A., and Muthuraman, K. (2011). American options under stochastic volatility. *Operations Research*, 59(4), 793–809 (<https://doi:10.1287/opre.1110.0945>).
14. Company, R., Egorova, V.N., and Jódar, L. (2016). A positive, stable and consistent front-fixing numerical scheme for American Options. Springer International Publishing AG 2016 (https://doi:10.1007/978-3-319-23413-7_10).
15. Company, R., Egorova, V., Jódar, L., and Vázquez, C. (2016). Computing American option price under regime switching with rationality parameter. *Computers & Mathematics with Applications*, 72 (3), 741–754 (<https://doi:10.1016/j.camwa.2016.05.026>).
16. Company, R., Egorova, V. N., and Jódar, L. (2016). Constructing positive reliable numerical solution for American call options: A new front-fixing approach. *Journal of Computational and Applied Mathematics*, 291, 422–431 (<https://doi:10.1016/j.cam.2014.09.013>).
17. Company, R., Egorova, V., Jódar, L., and Vázquez, C. (2016). Finite difference methods for pricing American put option with rationality parameter: Numerical analysis and computing. *Journal of Computational and Applied Mathematics*, 304, 1–17 (<https://doi:10.1016/j.cam.2016.03.001>).
18. Cont, R. and Tankov, P. (2004). Financial Modelling with Jump Diffusion. Chapman & Hall, London.
19. Crank, J. (1984). Free and moving boundary problem, Oxford University Press, London.
20. Dremkova, E. and Ehrhardt, M. (2008). A high-order compact method for non-linear Black-Scholes option pricing equation of American options. *International Journal of Computational Mathematics* 00 (00), 1-18.

21. Düring, B., and Fournié, M. (2012). High-order compact finite difference scheme for option pricing in stochastic volatility models. *Journal of Computational and Applied Mathematics*, 236 (17), 4462–4473 (<https://doi:10.1016/j.cam.2012.04.017>).
22. Egorova, V. N., Company, R., and Jódar, L. (2016). A new efficient numerical method for solving American option under regime switching model. *Computers and Mathematics with Applications*, 71 (1), 224–237 (<https://doi:10.1016/j.camwa.2015.11.019>).
23. Elliott, R. J., Siu, T. K., Chan, L., and Lau, J. W. (2007). Pricing options under a generalized markov-modulated jump-diffusion model. *Stochastic Analysis and Applications*, 25 (4), 821–843.doi:10.1080/07362990701420118 .
24. Gao, G. and Sun, Z. (2012). Compact difference schemes for heat equation with Neumann boundary condition (II). Wiley Online Library.
25. Garnier, J., and Sølna, K. (2017). Correction to Black–Scholes formula due to fractional stochastic volatility. *SIAM Journal on Financial Mathematics*, 8 (1), 560–588 (<https://doi:10.1137/15m1036749> Stochastic Volatility Correction to Black-Scholes).
26. Guoqing, Y., and Hanson, F. B. (2006). Option pricing for a stochastic-volatility jump-diffusion model with log-uniform jump-amplitudes. *American Control Conference*, (<https://doi:10.1109/acc.2006.1657175>).
27. Hamilton, J. D. (1989). A New Approach to the Economic Analysis of Nonstationary Time Series and the Business Cycle. *Econometrica*, 57 (2), 357 (<https://doi:10.2307/1912559>).
28. Han, Y., and Kim, G. (2016). Efficient lattice method for valuing of options with barrier in a regime-switching model. *Discrete Dynamics in Nature and Society*, 2016, 1–14 (<https://doi:10.1155/2016/2474305>).
29. Hirsch, C. (2001). *Numerical Computation of Internal and External Flows: Fundamental of Numerical Discretization*. Wiley, New York.
30. Huang, Y., Forsyth, P. A., and Labahn, G. (2011). Methods for Pricing American Options under Regime Switching. *SIAM Journal on Scientific Computing*, 33 (5), 2144–2168 (<https://doi:10.1137/110820920>).
31. Hull, J. and White, A. (1987). The pricing of options on assets with stochastic volatilities. *The journal of finance*, 42 (2), 281-300.
32. Ikonen, S., and Toivanen, J. (2007). Efficient numerical methods for pricing American options under stochastic volatility. *Numerical Methods for Partial Differential Equations*, 24 (1), 104–126 (<https://doi:10.1002/num.20239>).

33. Kangro, R., and Nicolaides, R. (2000). Far Field Boundary Conditions for Black--Scholes Equations. *SIAM Journal on Numerical Analysis*, 38 (4), 1357–1368 (<https://doi:10.1137/s0036142999355921>).
34. Khaliq, A. Q. M., and Liu, R. H. (2009). New numerical scheme for pricing American option with regime-switching. *International Journal of Theoretical and Applied Finance*, 12 (03), 319–340 (<https://doi:10.1142/s0219024909005245>).
35. Khaliq A. Q. M., Kleefeld, B., and Liu, R. H. (2013). Solving complex PDE systems for pricing American options with regime-switching by efficient exponential time differencing schemes. *Numerical Methods Partial Differential Equation*, 29 (1), 320-336.
36. Kou, S. G. (2002). A jump-diffusion model for option pricing. *Management Science*, 48 (8), 1086–1101 (<https://doi:10.1287/mnsc.48.8.1086.166>).
37. Kwok Y. K. (2008). *Mathematical models of financial derivatives*. Springer, Berlin.
38. Landau, H. G. (1950). Heat conduction in a melting solid. *Quarterly of Applied Mathematics*, 8 (1), 81–94 (<https://doi:10.1090/qam/33441>).
39. Li, H., Mollapourasi, R., and Haghi, M. (2018). A local radial basis function method for pricing options under the regime switching model. *Journal of Scientific Computing*, 79, 517-541.
40. Liao, W., Zhu, J., Khaliq, A. Q. M. (2002). *An efficient high-order algorithm for solving systems of reaction-diffusion equations*. Wiley Periodicals, Inc.
41. Liao, W. and Khaliq, A. Q. M. (2009). High-order compact scheme for solving nonlinear Black-Scholes equation with transaction cost. *International Journal of Computer Mathematics* 86 (6), 1009-1023 (<https://doi:10.1080/00207160802609829>).
42. Liu, R. H. (2010). Regime-switching recombining tree for option pricing. *International Journal of Theoretical and Applied Finance*, 13, 479-499.
43. Liu, R. H., Zhang, Q., and Yin, G. (2006). Option pricing in a regime-switching model using the fast Fourier transform. *Journal of Applied Mathematics and Stochastic Analysis*, 1–22 (<https://doi:10.1155/jamsa/2006/18109>).
44. Mamon, R. S., and Rodrigo, M. R. (2005). Explicit solutions to European options in a regime-switching economy. *Operations Research Letters*, 33 (6), 581–586 (<https://doi:10.1016/j.orl.2004.12.003>).
45. Meyer, G. H. and van der Hoek, J. (1997). The evaluation of American options with the method of lines. *Advances in Futures and Options Research*, 9 (9), 265–285.

46. Mitchell, S. L., and Vynnycky, M. (2009). Finite-difference methods with increased accuracy and correct initialization for one-dimensional Stefan problems. *Applied Mathematics and Computation*, 215 (4), 1609–1621 (<https://doi:10.1016/j.amc.2009.07.054>).
47. Mitchell, S. L., and Vynnycky, M. (2012). An accurate finite-difference method for ablation-type Stefan problems. *Journal of Computational and Applied Mathematics*, 236 (17), 4181–4192 (<https://doi:10.1016/j.cam.2012.05.011>).
48. Morton, W.K. and Mayer, D. (2005). *Numerical Solutions of Partial Differential Equations*. Cambridge University Press, London.
49. Nielsen, B. F., Skavhaug O., and Tveito (2002). A penalty and front-fixing methods for the numerical solution of American option problems. *Journal of Computational Finance*, 5 (4), (<https://10.21314/jcf.2002.084>).
50. Norris, J. R. (1998). *Markov Chain*. Cambridge University Press, London.
51. [Shang](#), Q., and Bryne, B., (2019). An efficient lattice search algorithm for the optimal exercise boundary in American options. *SSRN Electronic Journal*.
52. Tauryawati, M. L., Imron, C., and Putri, E. R. (2018). Finite volume method for pricing European call option with regime-switching volatility. *Journal of Physics: Conference Series*, 974, (<https://doi:10.1088/1742-6596/974/1/012024>).
53. Toivanen, J. (2010). Finite difference methods for early exercise options. *Encyclopedia of Quantitative Finance*, (<https://doi:10.1002/9780470061602.eqf12002>).
54. Ugur, O. (2009). *Introduction to Computational Finance*. Imperial College Press, London. (<https://doi.org/10.1142/p556>).
55. Wu, L. and Kwok, Y.K. (1997). A front-fixing method for the valuation of American option, *J. Finance. Eng.* 6 (2), 83–97.
56. Yan, Y., Dai, W., Wu, L., and Zhai, S. (2019). Accurate gradient preserved method for solving heat conduction equations in double layers. *Applied Mathematics and Computation* 354, 58-85.
57. Zhang, K., Teo, K. L., and Swartz, M. (2013). A Robust numerical scheme for pricing American options under regime switching based on penalty method. *Computational Economics*, 43 (4), 463–483 (<https://doi:10.1007/s10614-013-9361-3>).
58. Zhao, J., Davidson, M., and Corless, R. M. (2007). Compact finite difference method for American option pricing. *Journal of Computational and Applied Mathematics* 206, 306-321.

59. Zhyl'yevskyy, O. (2009). A fast Fourier transform technique for pricing American options under stochastic volatility. *Review of Derivatives Research*, 13 (1), 1–24 (<https://doi:10.1007/s11147-009-9041-6>).